Methods for Analyzing Submerged Jet Erosion Test Data to Model Scour of Cohesive Soils

T. L. Wahl

Published in *Transactions of the ASABE* 64(3): 785-799 (doi: 10.13031/trans.14212).

Submitted for review on 17 July 2020 as manuscript number NRES 14212; approved for publication as a Research Article by the Natural Resources & Environmental Systems Community of ASABE on 26 January 2021.

The author is **Tony L. Wahl,** Technical Specialist, Hydraulics Laboratory, U.S. Department of the Interior, Bureau of Reclamation, Technical Service Center, P.O. Box 25007, Denver, CO 80225-0007; phone: 303-445-2155; e-mail: twahl@usbr.gov.

Highlights

- *Fifty-two jet erosion tests performed on four cohesive soils were analyzed by nine different methods.*
- *Nonlinear methods performed well on some individual tests but fit inconsistently overall.*
- *Several alternate linear solution methods outperformed the widely used Blaisdell method.*
- *Simple linear regression of erosion rate versus applied shear stress provided the most consistent relationship between erosion rate and critical shear stress parameters.*

Abstract*. The submerged jet erosion test (JET) is widely used in lab and field settings to quantify erodibility of cohesive soils and determine erosion rate coefficients and critical shear stress values. Test devices with different scales and configurations have been developed in recent years, along with several alternative methods for processing the collected data to determine parameters of linear and nonlinear soil erosion equations. To facilitate standardization, 52 JET experiments were conducted on four different cohesive soils compacted at optimum water content and 2% dry and wet of optimum. Each test was analyzed using nine different methods, four based on the linear excess*

stress equation (including the commonly used Blaisdell method) and five based on nonlinear erosion equations, including two using the recently popular Wilson model. Results were analyzed to determine the erosion equations and parameter-fitting methods that most effectively represent the observed erosion rates and are of greatest utility for soil erosion modeling and the ranking and classification of soils according to erodibility. Methods based on nonlinear erosion equations fit some data sets well, but they exhibited poor correlation between the erosion rate coefficient and the threshold shear stress parameter for initiating erosion, which is problematic for soil erodibility classification work. Linear methods that simultaneously optimized erosion equation parameters to best fit the total depth of scour or the elapsed time needed to reach specific depths of scour performed better than the Blaisdell method, which has been the informally accepted standard of practice since the late 1990s. However, they also exhibited weak correlation of the erosion rate and critical shear stress parameters. Simple linear regression of average scour rate versus average applied stress provided an effective method for representing the erosion rate versus applied stress curve and exhibited the strongest correlation of the erosion rate coefficient and critical shear stress parameters.

Keywords. Cohesive soil, Critical shear stress, Erodibility, Erosion, Erosion laws, Erosion models, Jet erosion test, Shear strss, Soil moisture.

Erosion of cohesive soils is a critical process in a diverse set of problems confronting civil and agricultural engineers, including embankment erosion and breach, earthen spillway erosion, streambank migration, river channel degradation, rill erosion, and bridge pier scour. Recently, models to predict the rate and extent of erosion for many of these applications have become more quantitative, computing erosion as a function of applied stress and soil erosion resistance parameters. Such models require soil erodibility to be defined numerically, and this has been accomplished by relating observed erosion to applied stresses in controlled tests that can be conducted in the laboratory or in the field. Soil erosion in many of these applications is viewed as a detachment-limited process, and erosion rates have often been modeled using the excess stress equation:

$$\varepsilon_r = k_d \left(\tau - \tau_c \right)^a$$

(1)

where e_r is the volumetric erosion rate, t is the applied shear stress, t_c is the critical shear stress needed to initiate erosion, k_d is the detachment rate coefficient, and a is a numerical exponent greater than zero. When applied stress is below the threshold value, no erosion occurs. The a exponent is often assumed to be 1.0, and in that case the model is described as the linear excess stress equation. The soil erodibility parameters t_c and k_d can be determined by laboratory or field-based testing using a variety of devices, including submerged jets (Hanson and Cook, 2004), flume tests (Erosion Function Apparatus, or EFA, developed by Briaud et al., 2001; SEDFLUME developed by McNeil et al., 1996), and tests that use internal erosion (Hole Erosion Test developed by Wan and Fell, 2004), although different devices often produce differing numerical values of the parameters (Wahl et al., 2008). Due to the possibility of nonlinear erosion behavior, it has always been advisable to conduct erosion testing in a stress range that is similar to the stresses expected in

the application of interest. When the range of applied stresses is large during a single application event, extrapolating linear behavior beyond the stress range used during testing can be problematic.

The submerged jet erosion test (JET) was developed for the purpose of defining erodibility in a quantitative way and has been a useful method for determining erodibility parameters and studying relations between erodibility and other soil properties (Hanson, 1996; Hanson and Hunt, 2007). Devices have evolved rapidly since the 1990s, becoming smaller and more practical for field use. Standard procedures for performing jet erosion tests and analyzing the collected data were first defined in ASTM Standard D5852 (ASTM, 1995). The test is performed by applying stress to the soil surface from a fixed, impinging, submerged water jet oriented normal to the soil surface. Depths of scour along the axis of the jet are recorded at time intervals that are short at the start of the test, while applied stresses are large, and longer at later times when applied stresses diminish (due to increased distance between the jet nozzle and the eroded soil surface). A typical test duration is a few minutes up to a few hours, with no definite requirement for total test time other than the need to obtain adequate data points to support fitting of the data to an erosion function.

Although values of k_d and τ_c could be obtained by simple linear regression of observed erosion rates versus calculated applied stresses (Cossette et al., 2012), most investigators have determined erodibility parameters by fitting the scour depth and scour time observations to values predicted by numerically integrating the linear excess stress erosion equation. This approach is intended to make the result less sensitive to variability of the instantaneous scour rates, which can be high due to the inherent heterogeneity of both naturally occurring and engineered (compacted) soils.

Methods for analyzing JET data have become more sophisticated over time. Hanson (1991) described analyzing the data to estimate a jet index analogous to the k_d rate coefficient in the linear excess stress equation, assuming that τ_c is zero, and this method is presented in ASTM Standard D5852. Hanson and Cook (1997, 2004) subsequently investigated several methods for estimating the erodibility parameters when τ_c was allowed to be nonzero. They had difficulty getting consistent results from a method that optimized k_d and τ_c simultaneously and instead recommended a procedure that has become known in the recent literature as the Blaisdell method. It uses a two-step process in which τ_c is estimated first, using a hyperbolic function developed by Blaisdell et al. (1981) to estimate the equilibrium depth of scour in plunge pools (the limit approached at infinite time), and setting τ_c to be the stress that would be applied by the jet at this scour depth. The detachment rate coefficient is then estimated in the second step of the process by fitting the observed times of specific scour depths to the times projected by equations relating dimensionless scour to dimensionless time. To facilitate the curve-fitting process, Hanson and Cook (2004) developed a relation for dimensionless scour versus dimensionless time by integrating the differential equation that relates erosion rate to applied stress, following the lead of Stein et al. (1993) and Stein and Nett (1997). Use of the linear excess stress equation to model cohesive soil erosion and the Blaisdell method to analyze JET data have been dominant in practice for most of the past two decades.

Alternatives to the Blaisdell method have been proposed during the last decade, with different solution processes, constraints, and optimization objectives. Simon et al. (2010) proposed an iterative method that started with the Blaisdell method results and then further optimized τ_c and k_d simultaneously, while limiting the maximum value of τ_c. Daly et al. (2013) proposed a scour depth method that also optimized τ_c and k_d simultaneously but minimized differences between the predicted and observed depths of scour recorded at specific times during a test. Both of these methods were developed partially in an effort to reduce the variability of results from the Blaisdell method while also obtaining a closer relation between predicted and observed erosion rates (even though optimization was based on elapsed time and accumulated scour depth).

Several investigators have proposed that cohesive soil erosion is a nonlinear process with different values of the *a* exponent, e.g., 1/2 (Van Damme and Riteco, 2018), 3/2 (Foster et al., 1977), 7/4 (Walder, 2016), or 2 (Partheniades, 1965), or with the exponent allowed to vary as another fitted model parameter. Recently, there has been especially strong research interest in the unique nonlinear model developed by Wilson (1993a), which exhibits double curvature of the erosion rate versus shear stress relation, with gradually accelerating erosion rates at low stresses transitioning into a linear region and finally a square root relation at high stresses. The Wilson model was developed mechanistically by considering flow, gravitational, and cohesive forces acting on individual particles, along with the statistical characteristics of flow turbulence. It is also a two-parameter model, with one parameter defining a reference stress for initiation of erosion and a second parameter defining the increase in the rate of erosion as stress is increased. Wilson (1993b) tested the model initially by using it to model erosion rates measured in rill erosion experiments on cohesive soils and to predict incipient motion of noncohesive soil particles (setting cohesion forces to zero). Al-Madhhachi et al. (2013a) used the Wilson model to analyze erosion of cohesive soils in flume tests and JETs, and Khanal et al. (2016a) applied it to hole erosion test (HET) data collected from tests of cohesive soils by Wahl et al. (2008). Criswell et al. (2016) applied the Wilson model to flume tests that measured scour rates of noncohesive gravels. While these investigations have shown that erosion data can be fit to the Wilson model, no study has conclusively shown that the Wilson model is generally superior to a linear model. Khanal et al. (2016a) incorporated the Wilson model into the Bank Stability and Toe Erosion Model (BSTEM) and reported good comparisons between the revised model and field measurements, but outputs from such a complex application model do not provide compelling proof of the correctness of the erosion model itself because other parts of the model can exert a significant influence.

The Problem

ASTM Standard D5852 for the submerged jet erosion test was last renewed in 2007 but has since been withdrawn without replacement. New standards are under consideration, but substantial development of both new devices and new data analysis methods has taken place since the original standard was issued. ASTM Standard D5852 described a relatively large device, with a 0.5 m diameter tank to submerge the test site, a 13 mm diameter nozzle, and a set of profiling pins to measure the detailed shape of the developed scour hole. Hanson and Cook (2004) used a smaller apparatus (described as the "original JET" in recent literature) with a 0.30 m (1 ft) diameter tank, a 6.35 mm diameter nozzle, and a single probe to measure the centerline scour depth. They also developed a device of similar size for use on inclined slopes (Hanson et al., 2002). The mini-JET device first used by Simon et al. (2010) and described in detail by Al-Madhhachi et al. (2013b) uses a 0.10 m (4 in.) tank and 3.175 mm nozzle. For this smallest device, some systematic differences have been found in comparisons to erodibility parameters obtained from the original JET; specifically, Simon et al. (2010) noted higher k_d values (presumably using the iterative method to analyze tests conducted by each device), while Al-Madhhachi et al. (2013b) found lower t_c values (using the Blaisdell method) and proposed an adjustment for mini-JET t_c test results.

Four data analysis methods are well represented in the current literature: the Blaisdell method (Hanson and Cook, 2004), the iterative method (Simon et al., 2010), the scour depth method (Daly et al., 2013), and the Wilson model (Al-Madhhachi et al., 2013a). The first three methods determine the k_d and t_c parameters of the linear excess stress equation, while the last method determines parameters of the nonlinear Wilson model. Partial motivation for development of the three latter methods has been the consistent observation that the Blaisdell method estimates very large equilibrium scour depths (the limit of projected scour after infinite time) with associated very small t_c values (e.g., Simon et al., 2010; Cossette et al., 2012; Daly et al., 2013; Khanal et al., 2016b). The accompanying k_d values are also high due to the apparent misrepresentation of the critical stress,

which yields relations of erosion rate and shear stress that can be inconsistent with the actual erosion rates observed during a test.

In contrast, the iterative and scour depth methods have been demonstrated by several investigators (Daly et al., 2013; Khanal et al., 2016a) to yield larger t_c values and larger k_d values, but this has also led to an observation that these values then lead to predictions of very high erosion rates if the erosion relation is extrapolated to higher stress ranges in application. This has led users to reduce the k_d value to compensate (e.g., Daly et al., 2015). Others have pursued the use of the Wilson model, which predicts at high stresses that the erosion rate becomes primarily a function of the square root of the applied stress, which effectively reduces erosion rates compared to extrapolation of the linear excess stress equation. However, to date, there is no JET-derived test data that confirm the square-root relation at higher stresses. Khanal et al. (2016a) demonstrated good agreement between the Wilson model and internal erosion rates observed in the Hole Erosion Test (HET) apparatus, but entrance and exit losses that were not accounted for in the HET analysis (Luthi, 2011; Riha and Jandora, 2015) create uncertainties about this conclusion.

For the current JET user, the present situation is anything but standardized. With ASTM Standard D5852 withdrawn, a variety of test devices available, and several data analysis methods in common use, it is still difficult to define and study soil erodibility in a quantitative way. Despite criticism, the Blaisdell method is still widely used, as are the alternatives, and the plethora of available methods complicates and hinders efforts to use the JET to understand soil erodibility. Studies by Daly et al. (2016), Khanal et al. (2016a), Criswell et al. (2016), and Khanal and Fox (2020) have used various linear methods (Blaisdell, iterative, scour depth) and the Wilson model to study the spatial variability of test results in the field and the variability of results as a function of test conditions (pressure head setting, observation time intervals, test duration, and *in situ* water content). All of these studies were made more complex and challenging to interpret by the fact that multiple methods of data analysis were being employed in parallel, and although it was not their purpose, none of these studies have led to a definitive recommendation of the best analysis method. Ultimately, it is not practical for the JET user to analyze data with four different methods and two fundamentally different erosion models in order to cover all bases.

Purpose

The purpose of this study is to give JET users an objective evaluation of the erosion models and methods that can be used to analyze erosion tests and apply results to real situations. First, basic concepts and historic observations are reviewed about the modeling of cohesive soil erosion using the linear excess stress model. Next, the Wilson model is presented and examined in a dimensionless form to illustrate its basic behavior and characteristics, especially in comparison to the linear excess stress model. Following this introduction, other models are considered, and methods of solving for model parameters are presented. Finally, a collection of JET data sets obtained from laboratory tests of remolded specimens of four soils compacted at three different moisture conditions is analyzed by several different methods to evaluate the quality of the fit between observed and predicted scour depths and erosion rates. The results of this analysis lead to recommendations on how to best perform and analyze jet erosion tests in the future.

Erosion Models

Modeling the erosion of cohesive sediments has been a topic of significant research interest for about 60 years. Hanson (1989) subdivided the early studies of the phenomenon into those focused on stable channel design and allowable shear stress (Dunn 1959; Smerdon and Beasley, 1959; Carlson and Enger, 1963; Lyle and Smerdon, 1965; Kamphuis and Hall, 1983) and those focused on

erosion rates at various stresses (Abdel-Rahman, 1962; Partheniades, 1965; Grissinger, 1966; Partheniades and Paaswell, 1968; Ariathurai and Arulanandan, 1978; Van Klaveren and McCool, 1987).

Partheniades and Paaswell (1968), as summarized by Hanson (1989), suggested that cohesive soil erosion exhibits three regions of behavior versus applied shear stress. Region I erosion occurs at a relatively slow rate at stresses less than the critical stress. Region II erosion occurs at an increasing rate in proportion to increasing stress; this is the erosion typically studied in most experimental work. Region III is typified by mass erosion when the applied shear stress exceeds the strength of the bed on a large scale, causing removal of blocks of soil rather than individual sediment particles. Partheniades (1965) showed flume test data exhibiting this three-region erosion relation, with slowly accelerating erosion rates at low stresses, linearly increasing erosion rates at moderate stresses, and a decreasing growth of erosion rates at high stresses. This bears similarity to the Wilson model mentioned earlier, which will be presented in more detail later in this section. Arulanandan et al. (1980) also described an excess stress concept and stated that it is common for plots of erosion rate versus applied stress to illustrate three zones of behavior: (1) gradual, (2) steeper, and (3) gradual again. They described fitting a linear model to the middle zone and using its zero-erosion intercept to define the critical shear stress.

Excess Stress Equation

The excess stress equation (eq. 1) has been used by many investigators of soil erosion, including Foster et al. (1977), Dillaha and Beasley (1983), Temple (1985), Hanson (1989), and Stein and Nett (1997). Foster et al. (1977) reported that the data of Partheniades (1965) on erosion rates of cohesive soil beds subjected to open-channel flow of saltwater supported values of the *a* exponent of 1.0 at low stresses, varying up to 2.0 at high stresses.

A similar equation with dimensional consistency for all values of the exponent is (Lin and Wu, 2013; Walder, 2016; Gao et al., 2019):

$$\varepsilon_r = K\left(\frac{\tau}{\tau_c} - 1\right)^a$$

(2)

with units of K being the same as those of e_r and the value of K indicating the erosion rate at $t = 2t_c$.

A common assumption has been that the *a* exponent is equal to 1, yielding the linear excess stress equation:

$$\varepsilon_r = k_d\left(\tau - \tau_c\right)$$

(3)

with the following customary units in the SI and Imperial systems:

e_r in m s^{-1} [ft h^{-1}]

k_d in (m s^{-1})/(N m^{-2}) = m^3 $(N{\cdot}s)^{-1}$ [(ft h^{-1})/(lb ft^{-2}) = ft^3 $(lb{\cdot}h)^{-1}$]

t and t_c in N m^{-2} [lb ft^{-2}].

It is common when using SI units to express the erosion rate in cm s^{-1} and k_d in cm^3 $(N{\cdot}s)^{-1}$, which requires the inclusion of a 10^{-4} conversion factor on the right side of equation 3.

The Wilson Model

Wilson (1993a) developed a mechanistically based model for predicting the detachment rate of cohesive soils and demonstrated its application (Wilson 1993b) to rill erosion data from the Watershed Erosion Prediction Project (WEPP) data set (Elliot, 1989). The basis for the model was an analysis of the free-body diagram of sediment particles and a prediction of the probability of sediment detachment, considering the probability distribution of turbulent stresses. The model developed by Wilson (1993a) included 16 different mechanistic parameters, which for application could be simplified to a three-parameter model expressed as:

$$\varepsilon_r = \frac{b_0\sqrt{\tau}}{\rho_d}\left(1 - e^{-e^{\frac{1.28}{c_v} - 0.5572 - \frac{b_1}{\tau}}}\right)$$

(4)

where ?$_d$ is the soil dry density, b_0 and b_1 are soil erodibility parameters, and c_v is a flow-related parameter, the turbulence coefficient of variation. In the form shown here, the erosion rate (e_r) has units of volume per unit time per unit area (Wilson computed the erosion rate on a mass basis).

Wilson (1993b) tested a further simplified two-parameter model by assuming $c_v = 0.36$, a value similar to that obtained by Einstein and El Samni (1949) from studies of hydrodynamic forces on rough channel boundaries. This simplifies equation 4 to:

$$\varepsilon_r = \frac{b_0\sqrt{\tau}}{\rho_d}\left(1 - e^{-e^{3-\frac{b_1}{\tau}}}\right)$$

(5)

Parameters b_0 and b_1 in equations 4 and 5 can be mechanistically defined, but determining them from these definitions requires knowing several soil particle or aggregate parameters that are difficult to estimate. As an alternative, Al-Madhhachi et al. (2013a) estimated the b_0 and b_1 parameters of specific soils from JET data. Comparing the Wilson model (eq. 5) and the linear excess stress equation (eq. 3), the b_0 parameter serves a similar function as k_d, indicating the rate of increase of erosion as stress is increased, and b_1 serves a similar function as t_c, determining the stress level at which significant erosion begins. Units of b_1 are stress, while units of $b_0/?_d$ are velocity per square root of stress. A useful rearrangement of equation 5 is:

$$\varepsilon_r = \frac{b_0\sqrt{b_1}}{\rho_d}\sqrt{\frac{\tau}{b_1}}\left(1 - e^{-e^{3-\frac{b_1}{\tau}}}\right)$$

(6)

In this form, the combination $b_0(b_1)^{0.5}/?_d$ has units of velocity (volumetric scour rate per unit area) and indicates the reference scour rate for approximately $t/b_1 = 1$.

To illustrate the behavior of the Wilson model, the two-parameter model is made dimensionless by dividing by the reference scour rate, and the resulting function is plotted in figure 1. There are three distinct regions: an initial nonlinear region in which the erosion rate increases slowly at first then more rapidly as stress is increased above zero, a linear region ranging from approximately $t/b_1 = 0.2$ to 0.6, and a final region in which the erosion rate is proportional to the square root of the total stress. This final region is predicted as a result of changes in the hydrodynamic conditions, not due

to changes in the mechanism of soil detachment (mass erosion) suggested by others (e.g., Partheniades and Paaswell, 1968). Notable features of the curve are:

- There is no true critical shear stress, as the erosion rate only drops to zero when t = 0, although for computational purposes it is practically zero for $t/b_1 < 0.11$.
- An effective critical shear stress can be estimated by extending the linear region curve back to an erosion rate of zero (about $t/b_1 = 0.19$).

Varying the c_v parameter in the three-parameter model will affect the transition from the initial to final regions. Increasing c_v flattens the slope of the linear region and extends it to higher dimensionless stresses. Reducing c_v steepens and compresses the linear region.

To exhibit all three regions of the Wilson model function, the range of shear stresses applied to a soil must vary by a factor of about 4, from $t/b_1 = 0.2$ to 0.8.

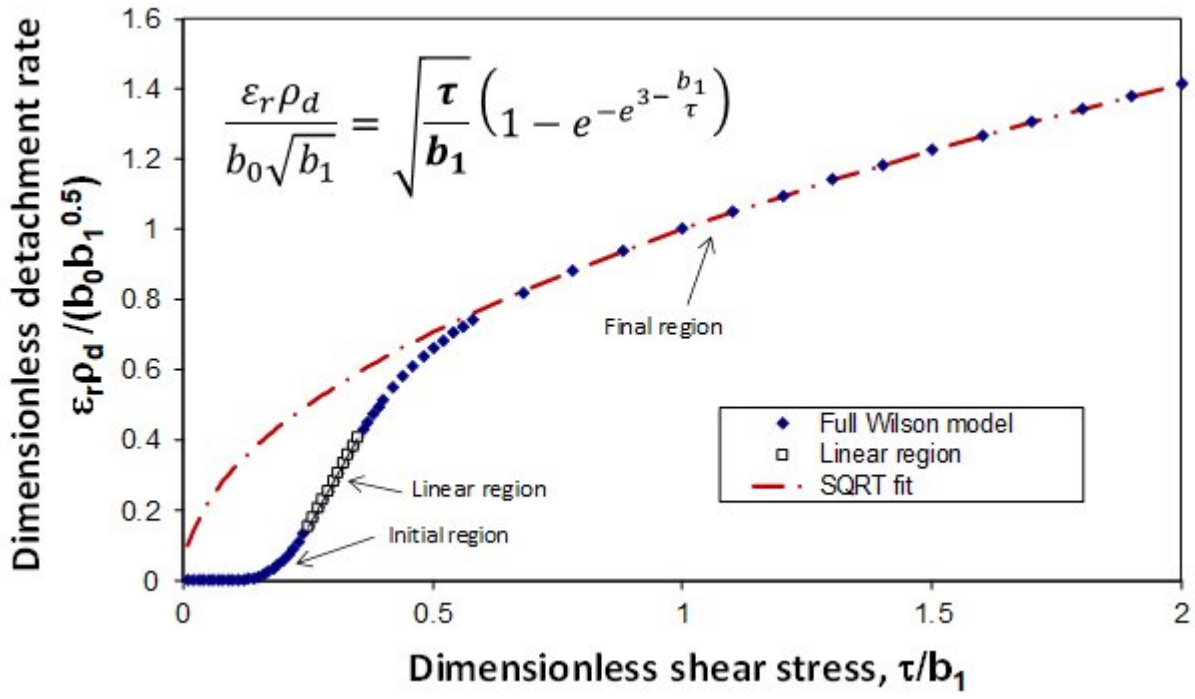

Figure 1. Dimensionless plot of Wilson model erosion rate function.

Exponential-Linear Model

An exponential-linear erosion model was developed during the present study, inspired by the Wilson model. It exhibits two erosion regions, an initial region with accelerating scour rate as shear stress is increased, followed by a linear region for higher stresses, as shown in figure 2:

$$\varepsilon_r = k_d \tau \left(\frac{e}{e-1} \right) \left(1 - e^{-e^{-\frac{b_1}{\tau}}} \right)$$

(7)

By including the numerical constant $e/(e\text{-}1)$, where e is the base of natural logarithms, the product of the two terms in parentheses approaches a limit of 1.0 for large values of t/b_1. This gives the relation a similarity to the linear excess stress equation, placing the effective x-intercept of a line fit through the low end of the linear region near $t/b_1 = 0.58$. At very high stress ratios, the function computes erosion rates that are proportional to total applied stress. Like the Wilson model, this function is theoretically nonzero for all positive stresses but is practically zero for $t < 0.2b_1$. Although this function is not derived from a mechanistic analysis, it empirically fits some data sets well and provides a relation that is consistent with many of the literature's descriptive accounts of the gradual, accelerating increase of erosion rate as shear stress is increased from low levels.

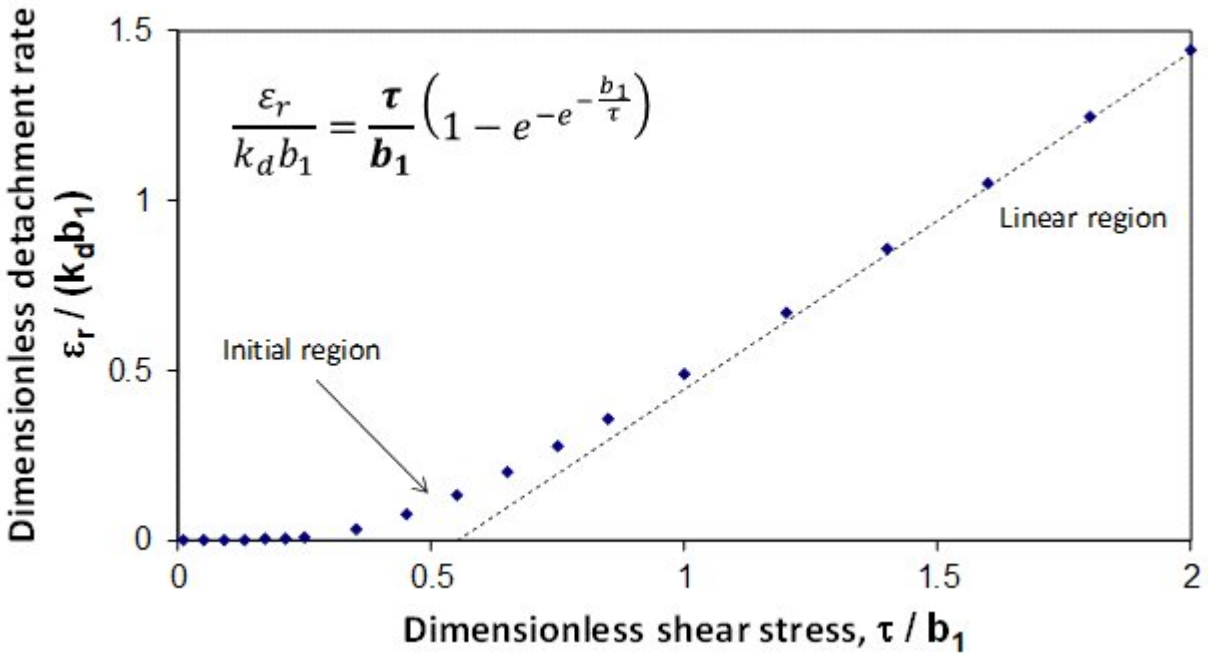

Figure 2. Exponential-linear erosion model.

Solution Methods

The linear excess stress equation and the Wilson model are both widely used in the recent JET literature, but a variety of solution methods (optimization schemes) are used to determine the

erodibility parameters that fit the test data to the models. Regardless of the curve-fitting methods, all approaches begin with the same estimation of the maximum shear stress applied to the soil specimen, using relations developed by Hanson et al. (1990) from hot-film measurements made beneath a submerged impinging jet in a smooth-bottomed tank with the same ratio of nozzle-to-tank diameter as that of the JET devices having 13 and 6.35 mm nozzles. The maximum stress has been experimentally found to occur at a small radial distance from the axis of the jet; however, in practice, the maximum scour typically occurs along the jet axis, and this measurement of scour is used for data analysis. Nguyen et al. (2017) proposed an analysis technique that uses additional scour measurements at points away from the center of the scour hole, and Marot et al. (2011) proposed an energy-based method that uses the measured volume of eroded material, but this study considered only the methods based on the centerline scour measurement. Hanson (1990) used a pin profiler to survey complete scour holes, but Hanson and Cook (1997) concluded that the centerline scour measurement provided a reliable index for analysis purposes.

Several different strategies and curve-fitting objectives can be used to optimize the erodibility parameters in the different erosion models. As described earlier, for the linear excess stress equation, Hanson and Cook (2004) presented what has come to be described in the literature as the Blaisdell method. It takes a two-step approach, estimating τ_c first using a hyperbolic logarithmic function (Blaisdell, 1981) to estimate the equilibrium depth of scour (the limit that would be approached at infinite time); once this depth is determined, τ_c is the stress that would be applied by the jet at this scour depth. The detachment rate coefficient is determined in the second step by fitting the observed times of specific scour depths to the times predicted by equations relating dimensionless scour to dimensionless time. Fitting is accomplished using Excel Solver, adjusting k_d to minimize the sum of squared errors between the observed and predicted dimensional times (not the related dimensionless variables). The fact that later data points during a test have relatively large numerical values of elapsed time causes the method to produce results that fit the later observations of scour better than the early observations.

Simon et al. (2010) proposed a method that uses the same optimization objective but uses Excel Solver to vary τ_c and k_d simultaneously to obtain the best fit. The method primes the initial values of the goal-seeking routine with the τ_c and k_d values obtained from the Blaisdell method and limits the maximum value of τ_c to the stress associated with the final scour depth recorded during a test. They called this approach the iterative method, but it is not apparent that the results are dependent on the exact starting values of τ_c and k_d; any values that lead Excel Solver to a successful optimization should produce the same end result. In this article, a solution technique using simultaneous optimization of the predicted times of specific observed scour depths is described as the "scour time solution."

Daly et al. (2013) developed a scour depth method that also solves simultaneously for τ_c and k_d but optimizes by minimizing the sum of squared errors between observed and predicted scour depths at the specific observation times used during a test. This method, like Simon's method, tends to produce larger τ_c and k_d values than the Blaisdell method. The skewness of the scour depth data is usually less than that of the scour times, so results tend to be less heavily weighted toward the data collected near the end of a test.

Al-Madhhachi et al. (2013a) determined the b_0 and b_1 parameters of the Wilson model for original JET, mini-JET, and flume erosion tests. Optimization was performed to minimize the sum of squared errors between observed and predicted erosion rates. Wilson (1993b) used a modified Gauss method to also minimize the sum of squared errors of the erosion rates when analyzing the WEPP rill erosion data set. Al-Madhhachi (2015, personal communication) indicated that an optimization method that minimizes errors in predicted scour depths has provided better data fits and has been

used for all of his subsequent work with the mini-JET and the Wilson model. In the present study, both scour rate and scour depth solutions were determined for the Wilson model.

Erodibility parameters k_d and b_1 for the exponential-linear model introduced in the previous section were also determined using both scour depth and scour rate optimization.

In addition to the methods just listed, two other solution approaches were applied in this study. First, a scour depth method based on the nonlinear excess stress equation was implemented. The solution was determined for each test by starting with the linear scour depth solution (a = 1) and then allowing Excel Solver to adjust K, t_c, and exponent a in equation 2. The final method determined k_d and t_c by direct linear regression of the plotted values of average applied shear stress and average erosion rate in each time interval of the tests. Cossette et al. (2012) used a similar approach in a comparison of different methods for determining t_c.

In summary, the following nine solution methods were applied to each data set:

- Linear excess stress, Blaisdell solution.
- Linear excess stress, scour time solution.
- Linear excess stress, scour depth solution.
- Linear excess stress, linear regression of scour rates.
- Nonlinear excess stress, scour depth solution.
- Wilson model, scour depth solution.
- Wilson model, scour rate solution.
- Exponential-linear model, scour depth solution.
- Exponential-linear model, scour rate solution.

Experiments

Fifty-two erosion tests were conducted with an original JET device on the four soils shown in table 1, prepared with standard Proctor compaction effort at three different nominal moisture conditions in standard 0.944 L (1/30 ft^3) Proctor soil molds. At least nine specimens were prepared and tested for each soil (table 2), three at optimum water content and three each at 2% dry and 2% wet of optimum conditions. Additional specimens were tested for some of the soils, including a total of 16 specimens for the sandy clay (SC) soil at 2% wet of optimum. This set of specimens was used to examine the behavior of this one soil over a broad stress range.

Table 1. Properties of tested soils and ASTM standards used to measure soil properties (ASTM, 2020).

USCS Soil Classification (ASTM D2487)	Particle Size Distribution (ASTM D7928)			Plasticity Index[a] (ASTM D4318)	Standard Compaction (ASTM D698A)	
	Clay (<2 µm) (%)	Silt (2 to 75 µm) (%)	Sand (>75 µm) (%)		?$_{d,max}$ (g cm^{-3})	WC$_{opt}$ (%)
Lean clay (CL)	40	53	7	25	1.67	20.3

Table 1. Properties of tested soils and ASTM standards used to measure soil properties (ASTM, 2020).

USCS Soil Classification (ASTM D2487)	Particle Size Distribution (ASTM D7928)			Plasticity Index[a] (ASTM D4318)	Standard Compaction (ASTM D698A)	
	Clay (<2 µm) (%)	Silt (2 to 75 µm) (%)	Sand (>75 µm) (%)		$?_{d,max}$ (g cm^{-3})	WC_{opt} (%)
Clayey sand (SC)	13	30	57	12	1.81	18.5
Silty clay (CL-ML)	8	83	9	7	1.69	17.0
Silty sand (SM)	12	27	61	Non-plastic	1.47	25.0

[a] Plasticity index is the difference between the liquid limit and plastic limit.

The soils were prepared by air drying, sieving through a U.S. No. 4 sieve (4.75 mm), remoisturizing to the desired water content, and then holding prior to compaction as prescribed by ASTM Standard D698A based on clay content. Specimens were machine-compacted using standard Proctor methods and compaction effort, and most were tested immediately or within a few hours after compaction. Akinola et al. (2018) showed that erosion resistance increases with the elapsed time between initial soil moisturization and jet testing, especially for soils with low clay content (e.g., SM), but we were initially unaware of this finding and did not begin tracking this time until late in the test program. Similarly, Akinola et al. (2019) showed that, irrespective of soil type, erosion rates increase as a function of the temperature difference between the eroding water and the soil specimen (i.e., hot water or cold soil leads to faster erosion). Again, we only began tracking these temperatures late in the test program. The water source for all tests was potable water from the laboratory's internal systems; based on recent monitoring of water and soil temperatures, we believe that most specimens were tested with water that was about 10°C to 12°C colder than the soil specimen. In a few instances, the temperature difference may have been smaller, about 5°C cooler than the soil.

Table 2. JET test parameters.

Soil	Number of JETs / Test Head (cm of water)		
	2% Dry	Optimum	2% Wet
CL	3 / 183	3 / 183	3 / 183
SC	4 / 91 to 183	4 / 183	16 / 91 to 366
CL-ML	4 / 36	3 / 36	3 / 36
SM	3 / 36	3 / 36	3 / 36 to 91

All soil specimens were compacted in three equal lifts, and the top of each specimen was trimmed after compaction of the third layer. Specimens were then inverted so that the bottom (untrimmed) surface was subjected to erosion during each JET. ASTM Standard D5852 describes field testing of *in situ* soils or laboratory testing of large (0.44 m diameter by 0.18 m high) undisturbed samples and suggests trimming both ends of laboratory samples; procedures for testing of remolded specimens are not addressed by the standard.

Three statistical measures were used to compare the goodness of fit of the different solution methods. The normalized objective function (NOF) used by Al-Madhhachi et al. (2013a) is the standard deviation of the N differences between observed (x_i) and predicted (y_i) values divided by the mean of the observations (X_a):

$$\mathrm{NOF} = \sum_{i=1}^{N} \frac{\left(x_i - y_i\right)^2}{N} / X_a$$

(8)

NOF values are always positive, with a better fit of predicted and observed values causing NOF to tend toward zero. Depending on the solution methods used, the observations could be of scour depth at a particular time, the elapsed time to reach a specific scour depth, or the average rate of erosion during a time interval of the test.

Values of the coefficient of determination (R^2) were also computed and used to compare the solution methods:

$$R^2 = 1 - \frac{SS_{res}}{SS_{tot}} = 1 - \frac{\sum_{i=1}^{N}\left(x_i - y_i\right)^2}{\sum_{i=1}^{N}\left(x_i - \overline{x}\right)^2}$$

(9)

where SS_{res} is the residual sum of squares, and SS_{tot} is the total sum of squares. Values of R^2 can vary from -8 to 1, with values near 1 indicating better fit of the predicted and observed values. The coefficient of determination can be inflated by a very wide or strongly skewed distribution of the observed values, more so than the NOF.

Finally, adjusted R^2 values were computed as:

$$R^2_{adj} = 1 - \left(1 - R^2\right)\frac{N-1}{N-p-1}$$

(10)

where N is the number of observations, and p is the number of parameters of the model. When a model with more parameters is used (such as the nonlinear excess stress model, which contains three parameters, compared to the two parameters of the linear excess stress model), an increase in the value of R^2_{adj} indicates that the additional parameter has added predictive value and an improved fit that exceeds what would have been expected just from random chance. Use of R^2_{adj} allows an unbiased comparison of models that have different numbers of fitted parameters.

Results

Linear Excess Stress

A comparison of the results from the four different solution methods applied to the linear excess stress model is shown in figure 3, mapped onto the k_d versus t_c space used by Hanson and Simon (2001) and others for the presentation of erodibility data and classification of soils into erodibility categories. As other investigators have found, the Blaisdell solution generally produces lower estimates of both t_c and k_d. Previous investigators (Hanson and Simon, 2001; Simon et al. 2010; Daly et al. 2013; Al-Madhhachi et al., 2013b) have suggested that correlation of k_d and t_c is a fundamental aspect of soil erodibility and have proposed several different regression relations between t_c and k_d, with the relation between them always having the form of a power curve (a linear fit on log-log scales). While determination of such relations was not the specific aim of this study, regression lines are plotted and it is notable that the simple linear regression approach has the smallest scatter and yields the highest R^2 value. The Blaisdell and scour depth solutions have similar R^2 values for the relation between t_c and k_d, while the scour time solution has a low value of R^2, impacted significantly by five results with exceptionally low values of t_c. These tests were all performed on the silty sand (SM) soil. Even if these five data points were excluded, the R^2 value for the results obtained from the scour time solution would only increase to about 0.42.

Figure 4 shows a comparison of the NOF statistics for the Blaisdell solutions of each JET experiment versus those of the linear scour time and scour depth solutions. The scour time solution has a lower NOF (better fit) than the Blaisdell solution for all tests. This is expected because both solutions use the same objective (minimizing squared errors of predicted scour times), and the scour time solution optimizes t_c and k_d simultaneously to minimize the objective function. The scour depth solution also has lower NOF values than the Blaisdell solution for most of the tests. Figure 5 compares the scour depth and scour time solutions and shows that the scour depth solution produces generally better fits, as indicated by a lower NOF value for the majority of the tests. There is not a convenient way to compare goodness-of-fit statistics for the linear regression of scour rates approach versus the other methods because they use different optimization objectives; if they were compared on the basis of predicted scour depths or scour times, the linear regression of scour rates

approach would be expected to exhibit poorer fits, but if they were compared on the basis of scour rates, the linear regression method would be superior by definition because it minimizes the squared errors of predicted scour rates.

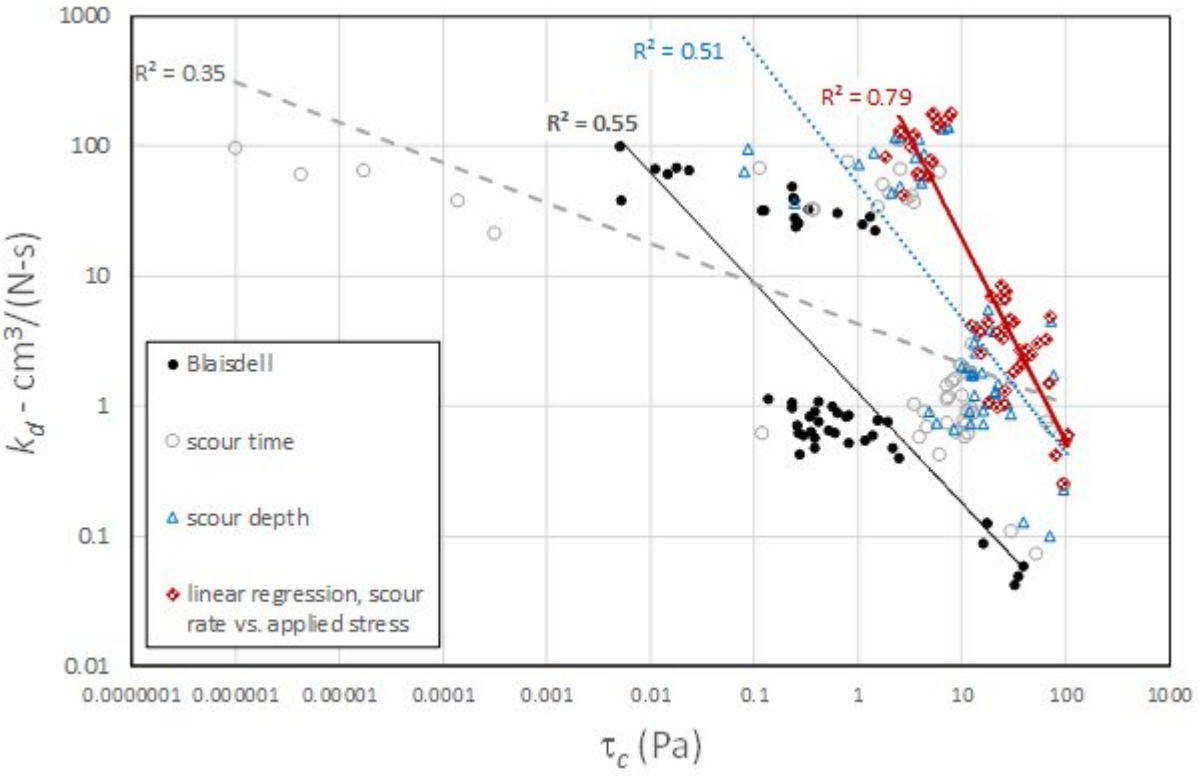

Figure 3. Relation of k_d versus t_c for solutions based on linear excess stress equation.

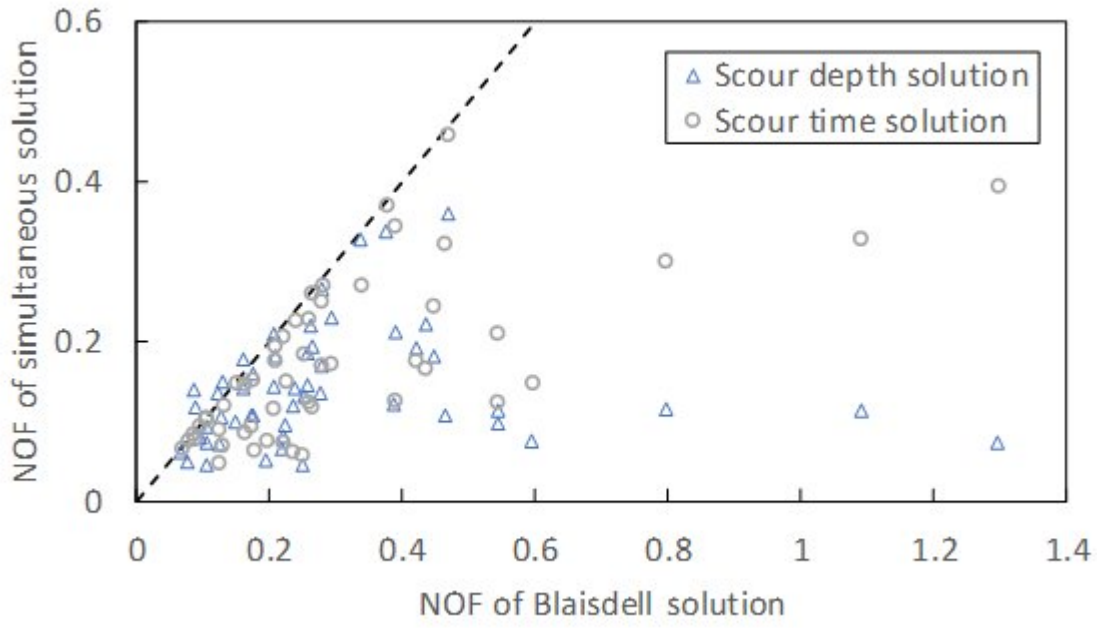

Figure 4. NOF comparison of Blaisdell method versus simultaneous solutions.

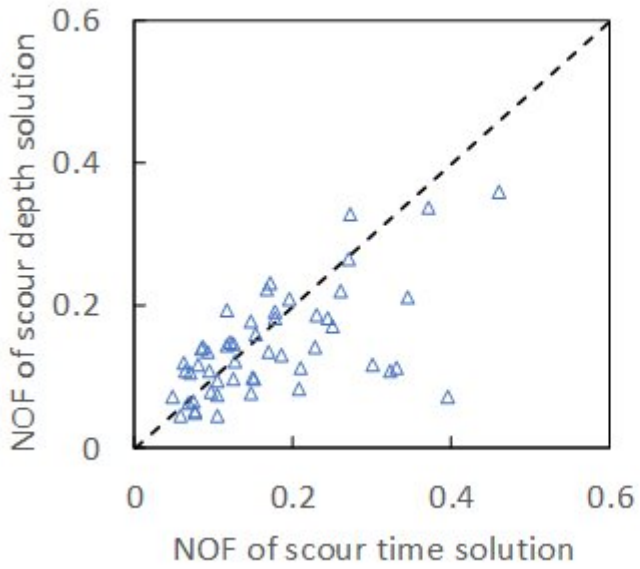

Figure 5. NOF comparison of scour depth versus scour time solutions of linear excess stress model.

Linear versus Nonlinear Excess Stress

Optimization of the nonlinear excess stress equation was performed using the scour depth method, beginning from the solution for the linear excess stress equation. The value of the a exponent was then varied (k_d and t_c were also allowed to adjust) to find the value that minimized the sum of squared differences between observed and predicted scour depths. By definition, the nonlinear solution must fit the data better because a third fitting parameter is used. Figure 6 compares the NOF and adjusted R^2 values of the linear versus nonlinear solutions and shows that even the adjusted R^2 values are better for the nonlinear solution in almost all cases.

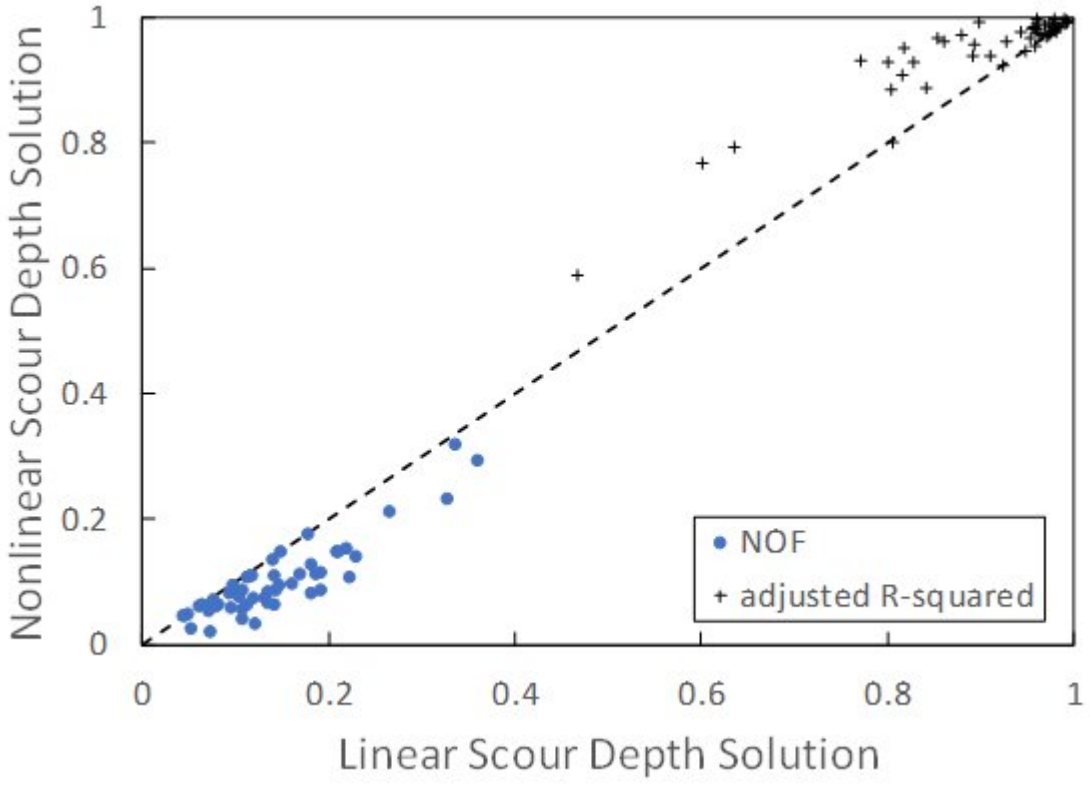

Figure 6. Goodness of fit for nonlinear versus linear excess stress solutions.

Although the nonlinear solution produces better fits of the scour depth data, figure 7 shows that the better fits are achieved primarily by adjustment of the *a* exponent to fit each individual test, and the result is a wide range of *a* values, scattered from slightly below 1 to almost 5, with no commonality or correlation to soil type or water content of the tested specimens. This suggests that although better fits to individual tests can be obtained using the nonlinear equation, there is no consistent value of the exponent. Even among the series of 16 tests that were performed on similar specimens of the SC soil near 2% wet of optimum, the values of the exponents for individual tests varied widely from about 1.1 to 2.7.

Wilson Model

The JET results were used to analyze the performance of the Wilson model compared to the linear excess stress equation and to consider whether the optimization of the Wilson model parameters should be based on a comparison of predicted versus observed scour depths or scour rates.

Figure 8 compares the NOF values obtained from scour depth solutions using the Wilson model and the linear excess stress equation, separated by soil type. In 79% of the cases, the linear excess stress equation provides a lower NOF value, indicating a better fit to the observed scour depths, and a comparison of adjusted R^2 values yields the same result. This is consistent with the observation from figure 7 that the exponents of the nonlinear excess stress equation were greater than 1 in almost all cases; in contrast, the Wilson model presumes that the erosion rates at high stresses will be proportional to the 0.5 power of applied stress. However, it is also possible for the Wilson model to be fit to the data using primarily the initial region curve (which behaves like an exponent greater than 1), avoiding the final region entirely, and a review of the individual JET results shows that this does happen in some cases.

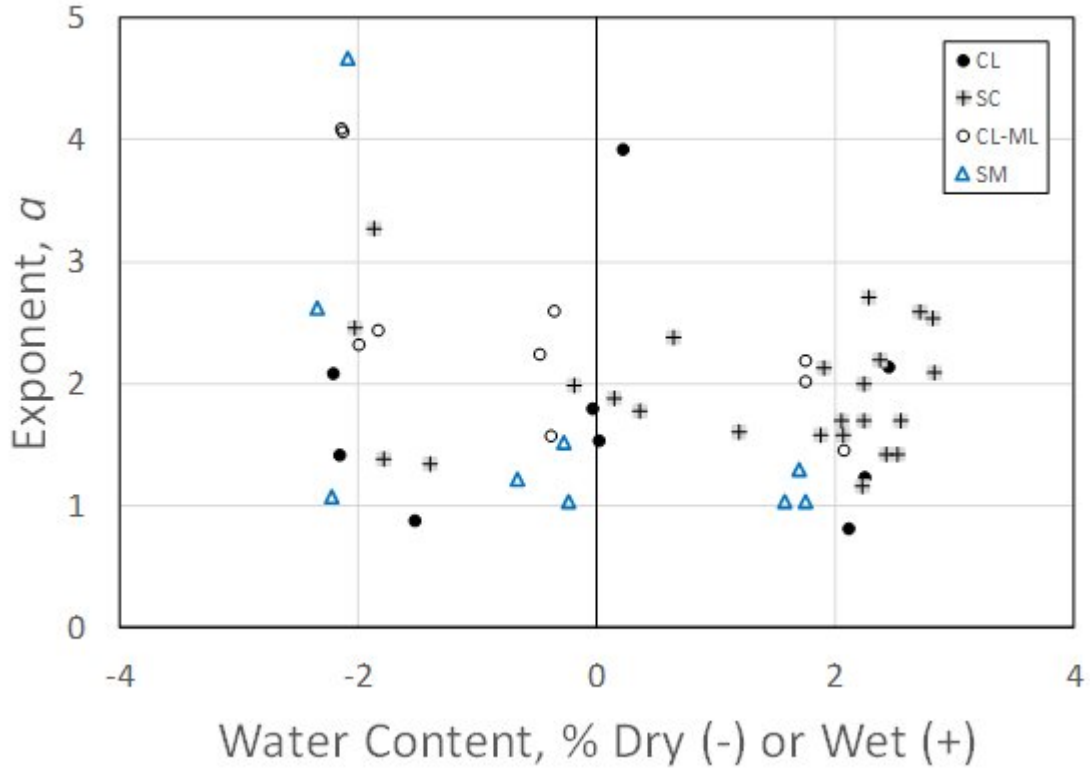

Figure 7. Fitted values of shear stress exponent (a) for nonlinear excess stress equation.

Comparing the NOF values in figure 9 for scour rate solutions shows an opposite result, with the Wilson model providing a superior fit to the erosion rate data in 77% of the tests. The question that remains is whether these results are being obtained due to the Wilson model's consistent ability to better represent real erosion behavior or by arbitrary overfitting of the model to nonlinearity that is present in the individual test data, but not necessarily indicative of consistent, real behavior.

As noted earlier, investigators have long observed that the k_d and t_c parameters of the linear excess stress equation are inversely related and have proposed various power curve equations relating them. Criswell et al. (2016) also suggested a power curve relation between the b_0 and b_1 parameters of the Wilson model, using values determined by a scour depth solution method for data from flume tests of four uniformly graded fine gravels. Gao et al. (2019) performed EFA tests of artificially constituted mixtures of a silty clay soil and uniform 5 to 6 mm gravel, at 10% increments of silty clay, and found an inverse relation between b_0 and b_1 values of the Wilson model, represented with two linear equations. (They were not specific about whether their determination of the b_0 and b_1 parameters was based on scour depths or scour rates.)

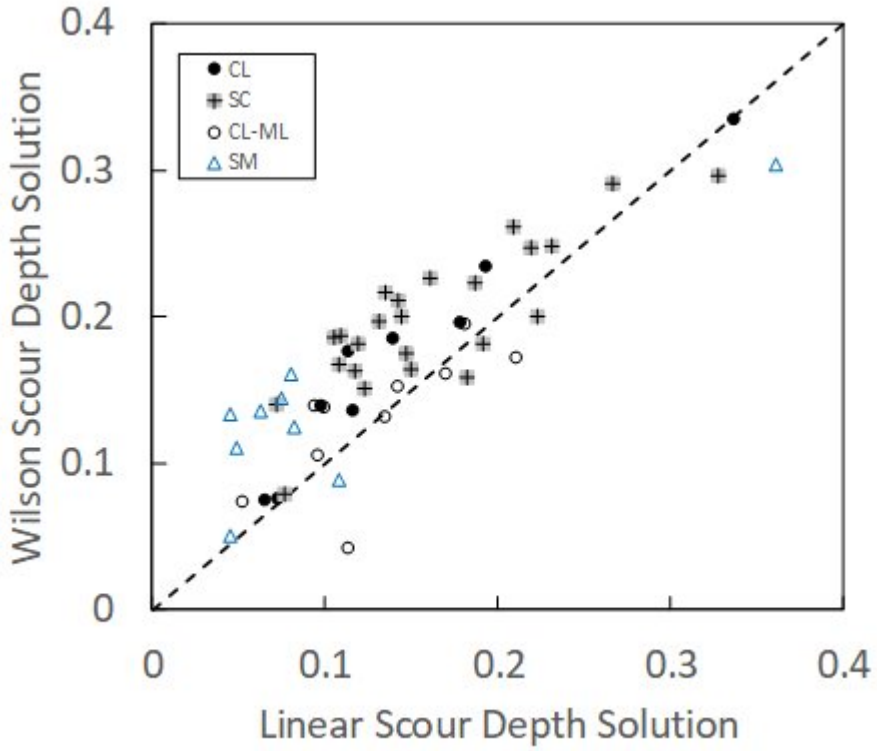

Figure 8. NOF values of scour depth solutions for Wilson model and linear excess stress equation.

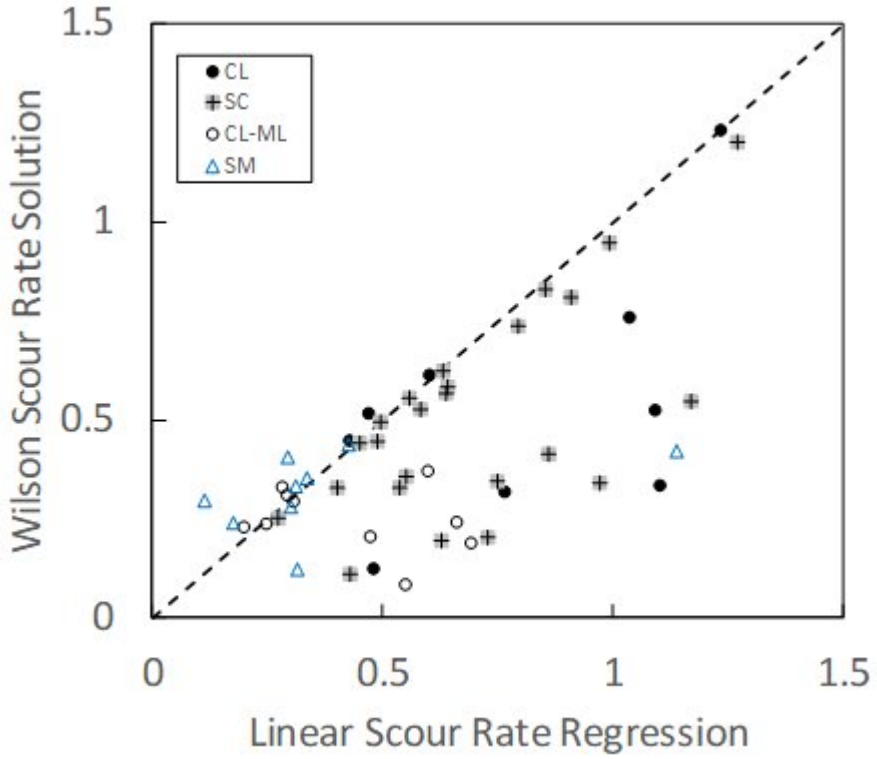

Figure 9. NOF values of Wilson model scour rate solution versus linear excess stress scour rate regression.

Figure 10 compares $b_0/?_d$ (a volumetric rate parameter, where $?_d$ is dry density) versus b_1 values for the scour depth and scour rate solutions of the Wilson model applied to the JETs conducted in the present study. The $b_0/?_d$ combination is used rather than b_0 itself because it is analogous to k_d and is

more readily available from *in situ* testing in which the dry density of the soil may not be known. There is a weak inverse relation between the parameters for the results obtained by scour depth optimization, with a fitted power curve equation having $R^2 = 0.22$. The results obtained by scour rate optimization exhibit no relation between the parameters ($R^2 = 0.00$), with b_1 varying by about three orders of magnitude while $b_0/?_d$ values are scattered across eight orders of magnitude. So, while the Wilson scour rate solution produces good curve fits to individual tests, the results have little value for characterizing erodibility over a range of soil conditions. Soils with similar thresholds for initiation of erosion would have wildly different erosion rates under increasing stress. This contradicts empirical observations that soils with high initial erosion resistance also erode at slower rates than those with less initial erosion resistance (e.g., Arulanandan et al., 1980; Briaud et al., 2001; Hanson and Simon, 2001; Wan and Fell, 2004). For comparison, recall that the results of the simple linear regression of scour rates and applied stresses yielded a power curve relation between k_d and t_c with an R^2 value of 0.79 (fig. 1). That behavior is consistent with empirical experience.

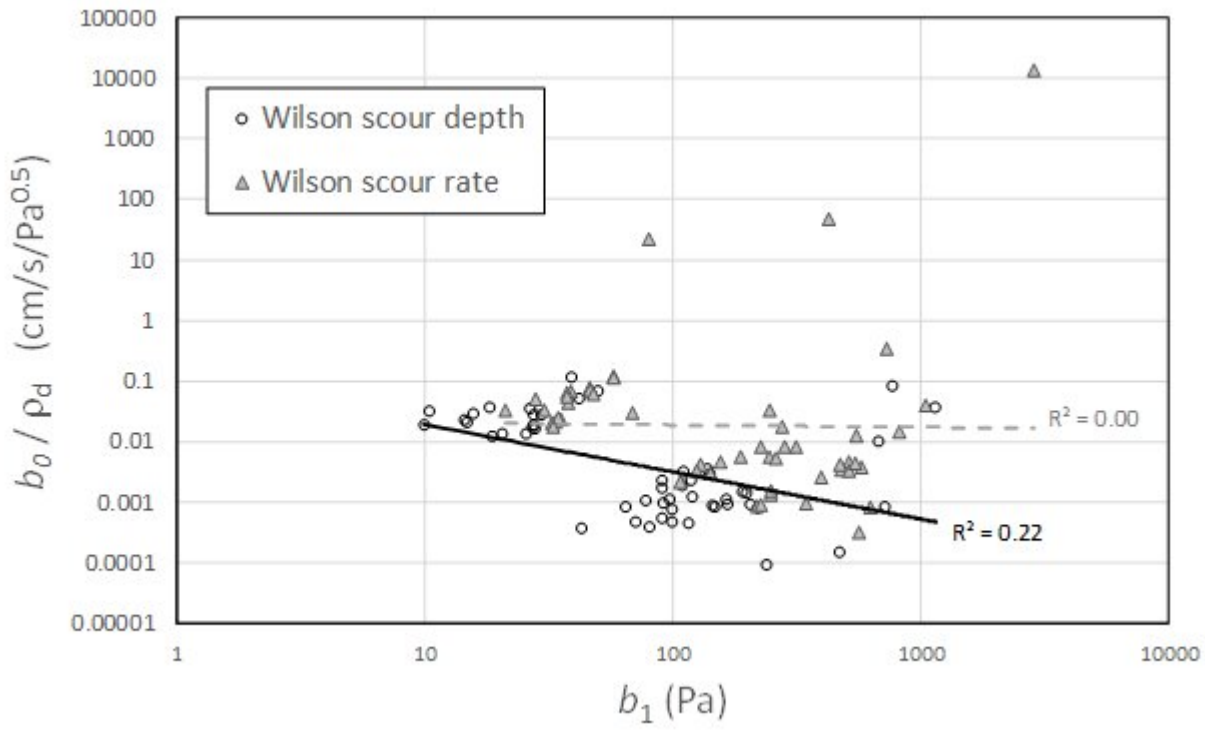

Figure 10. Erosion rate versus erosion threshold parameters of Wilson model.

Wilson Model Final Region Tests

Some individual tests had very low NOF values for the Wilson scour rate solution and produced scour rate versus shear stress plots that appeared to be very well fit, such as tests 3 and 6 of the SC soil compacted 2% wet (fig. 11). However, these tests only provided data to define the initial and linear regions; the final region curve at high stresses (above about 75 Pa) was completely extrapolated.

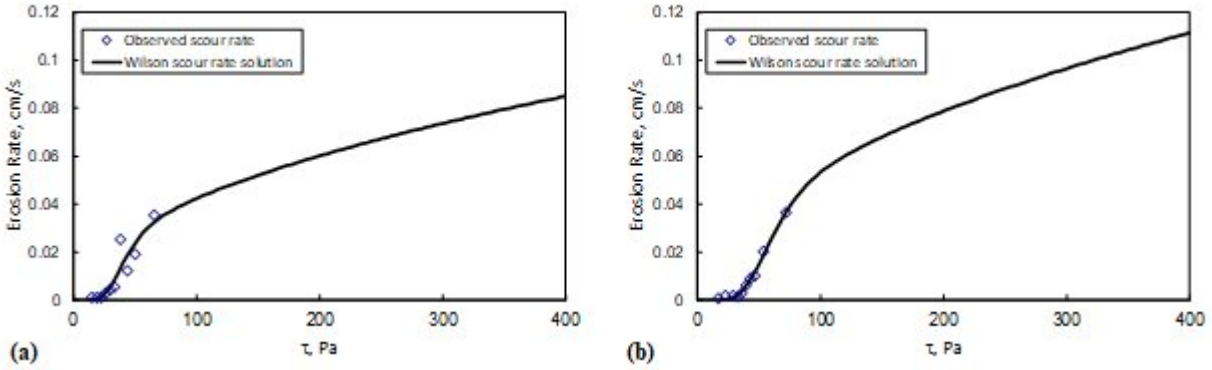

Figure 11. Observed scour rates and fitted Wilson model curves for (a) test 3 and (b) test 6 of the SC soil compacted 2% wet of optimum. NOF values were 0.44 and 0.11, respectively.

To test whether the Wilson model could also define the final region, additional tests of this soil were performed at higher pressure head settings that would produce larger initial shear stresses and allow a wider range of stresses to be applied in each test. Figure 12 shows that the additional tests did not define the final region consistently and tended to produce new Wilson model curves that exhibited larger values of the reference stress b_1. Wilson model curves again fit the data through the initial and linear regions but seldom contained more than one data point that even began to define the final region, which was still largely extrapolated from the fit to the initial and linear region data. The resulting b_0 and b_1 parameters for these individual tests produced widely varying extrapolated curves for the final region, with a 16-fold spread in projected erosion rates at a stress of 400 Pa.

Comparing the curves and erosion rate data points shown in figures 11 and 12, the tests run at higher heads tended to exhibit erosion rates varying within the 0 to 0.1 cm s^{-1} range for shear stresses in the range of about 100 to 300 Pa, whereas the tests at lower heads exhibited similar erosion rates when shear stresses were in the range of 25 to 75 Pa. The high-head tests performed at 3.66 m of head also exhibited very low erosion rates (Wilson model initial region behavior) when stresses decreased below about 100 Pa, whereas the low-head tests performed at 0.9 and 1.8 m of head exhibited low erosion rates for stresses below about 25 Pa. These differences may be due to fundamental changes in the erosion process when higher shear stresses are applied, such as a tendency to detach larger-scale aggregations of cohesive particles. This reinforces the point that erosion testing should always be performed with applied stresses in the range of those expected to occur in the real-world application of interest.

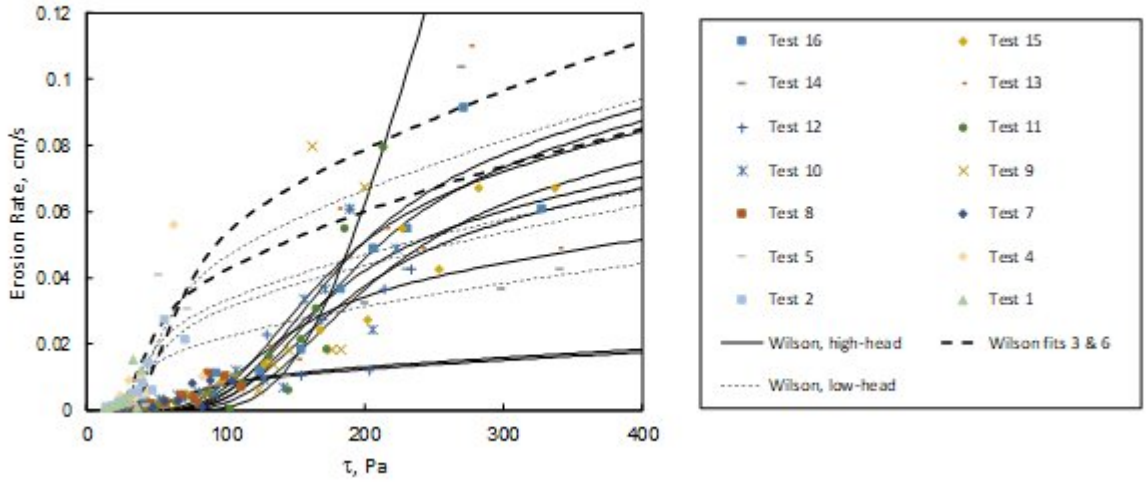

Figure 12. Erosion rate data and Wilson model curve fits for ten high-head JETs (tests 7 to 16) and six low-head JETs (tests 1 to 6) of the SC soil compacted 2% wet of optimum.

Exponential-Linear Model

The exponential-linear model was fit to each of the 52 JET data sets, optimizing separately for scour depth and scour rate prediction. Results were compared to the linear scour depth and Wilson scour depth results, and the scour rate linear regression and Wilson scour rate solutions.

Figure 13 shows that the exponential-linear model produces scour depth predictions that are better in almost all cases (lower NOFs) than those obtained from the linear excess stress model. Because the linear excess stress method outperformed the Wilson scour depth solution, the exponential-linear model also outperforms it.

Figure 14 shows that the scour rate solutions from the exponential-linear model were also superior in most cases to the linear regression of scour rates. The Wilson model also outperformed linear regression for most cases. Figure 15 shows that the exponential-linear and Wilson model NOF values are similar in most cases.

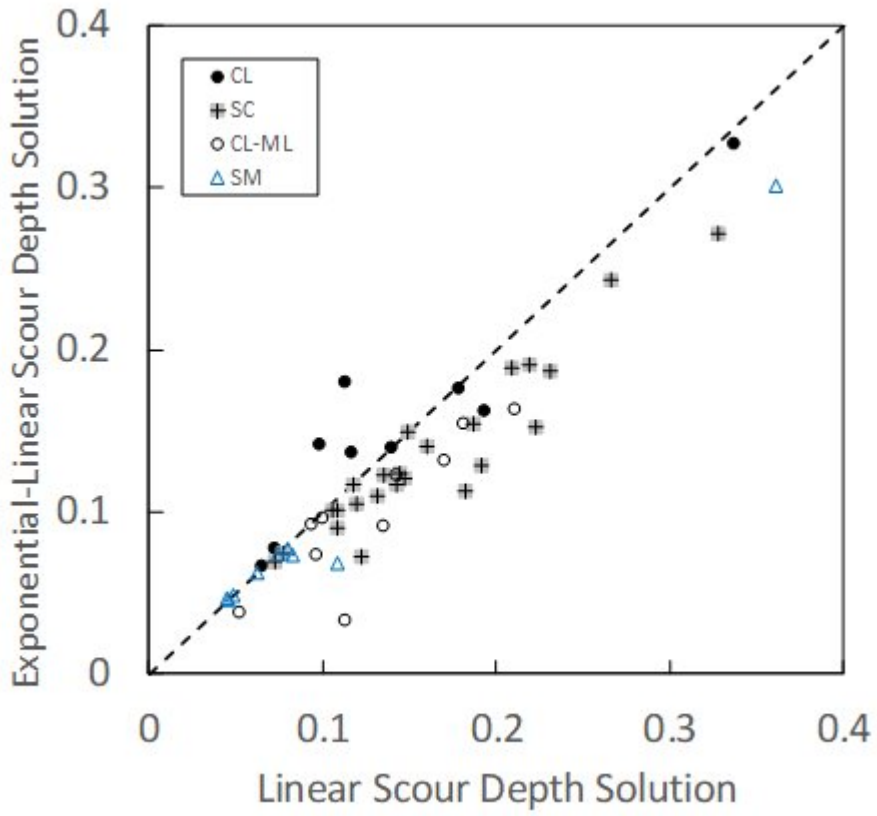

Figure 13. Comparison of NOF values for exponential-linear scour depth solution and linear scour depth solution.

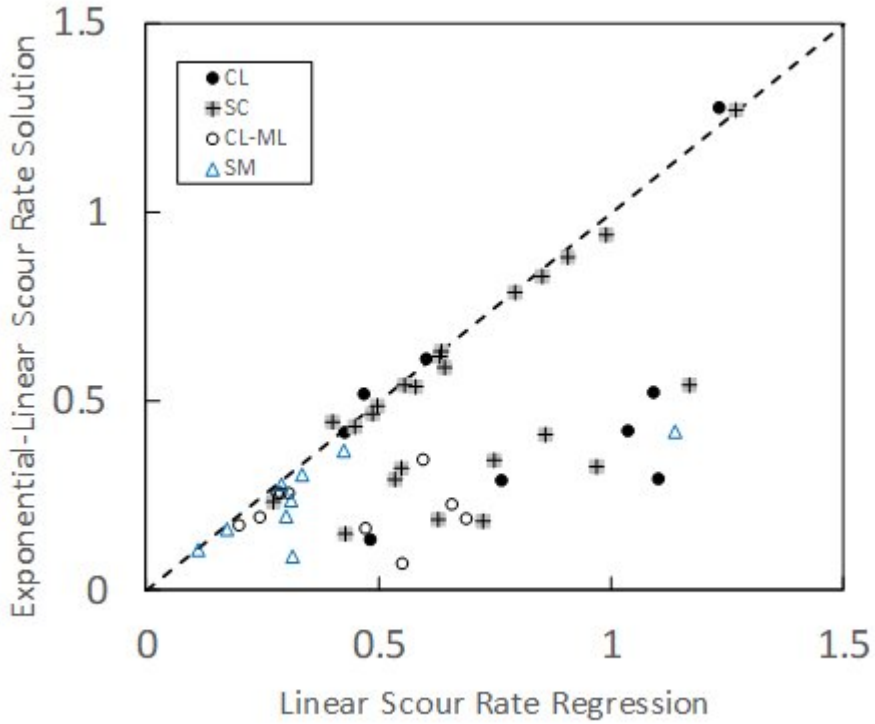

Figure 14. Comparison of NOF values for exponential-linear scour rate solutions versus linear excess stress model regression results.

As done with the previously tested models, figure 16 examines whether the exponential-linear model provides a consistent relation between the erosion rate and critical shear stress parameters. The figure compares k_d versus b_1 values for the scour depth and scour rate solutions of the exponential-linear model. Relations in both cases are very weak, with R^2 values only slightly above zero. Values of k_d vary over four or five orders of magnitude and value of b_1 vary over five to ten orders of magnitude.

Discussion

This research considered several methods for determining parameters of the linear excess stress equation and alternative nonlinear erosion models. The questions of whether nonlinear models are beneficial and which methods of solution are most useful must both be considered.

The Wilson model is the most commonly cited nonlinear erosion model in recent JET literature. Some previous investigators have suggested that it provides superior fits to observed JET data. This study showed that the Wilson model optimized to match scour depth data did not perform as well as the linear excess stress equation optimized in a similar way (fig. 8), but it outperformed the linear model in individual cases when optimized to fit scour rates (fig. 9). However, correlations between the rate parameter and shear stress threshold parameter across multiple tests were poor for the Wilson model, regardless of which optimization method was used (fig. 10). Some data sets were obtained that exhibited good definition of the initial and linear regions of the Wilson model (fig. 11), but no consistent definition of the final region could be obtained (fig. 12), and erosion rates at high stresses had to be largely extrapolated from the behavior in the initial and linear regions. These observations indicate that although the Wilson model may provide a good numerical fit to some individual tests, it does not provide results that are consistent with broadly accepted empirical experience that soils with high initial erosion resistance also erode at slower rates. This fundamental

contradiction with real-world behavior indicates that the Wilson model cannot be reliably used to rank and classify soils with regard to their erodibility, nor to model their behavior numerically.

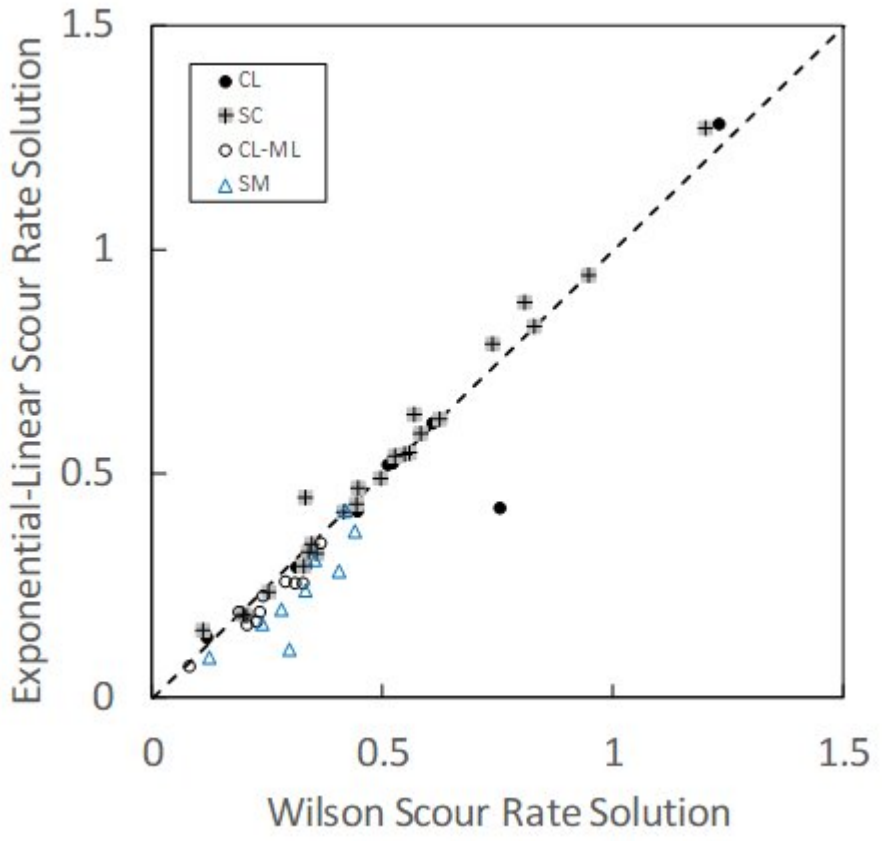

Figure 15. Comparison of NOF values for exponential-linear scour rate solutions versus Wilson model scour rate solutions.

The exponential-linear model proposed during this study outperformed the linear excess stress equation for individual tests when optimized for scour depth (fig. 13) and scour rate (fig. 14). It performed similarly to the Wilson model when optimized based on scour rate (fig. 15). Unfortunately, correlations between the rate parameter and shear stress threshold parameter across multiple tests were again poor for both optimization methods (fig. 16). The lack of consistent correlation of the rate and threshold parameters greatly diminishes the utility of either of these nonlinear erosion models, especially for the purpose of classifying soils into erodibility groups (very erodible, erodible, resistant, very resistant, etc.) because different classifications would be assigned depending on whether one focused on erosion rate or resistance to erosion initiation.

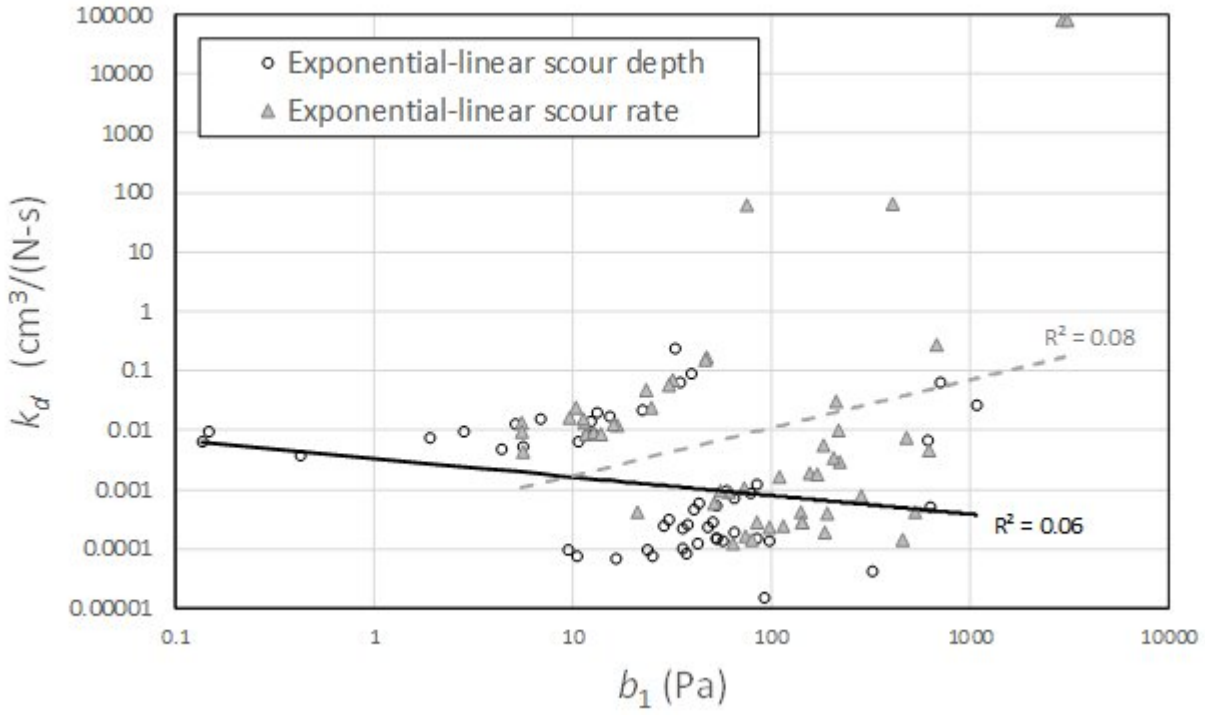

Figure 16. Erodibility parameter relationships for exponential-linear models optimized for scour depth and scour rate prediction.

The nonlinear excess stress equation was only tested using optimization based on scour depth data and, as expected, was able to produce better fits to individual JET data sets than the scour depth solution of the linear excess stress equation. However, values of the *a* exponent varied greatly and exhibited no useful correlation to other soil parameters. It seemed that the value of *a* was often overfitted to noise in the JET data sets.

Parameters of the linear excess stress equation were determined by the Blaisdell method, which estimates t_c and k_d in separate steps, and by simultaneous adjustment of both parameters to optimize predicted scour times and scour depths. The scour time method can be compared most readily to the Blaisdell method because the optimization objective is similar, and figure 4 shows that it significantly outperforms the Blaisdell method with much lower NOF values in most cases. The scour depth method generally outperforms the scour time method when NOF values of individual tests are compared (fig. 5), although it must be kept in mind that the basis for calculation of these NOF values is different (scour time versus scour depth).

The most direct solution method tested in this study is the linear regression of average scour rate versus average applied stress for each time interval. The fitted parameters can be calculated directly, without the need for optimization using Excel Solver. NOF values for the linear regression results cannot be directly compared to the NOF values obtained from the Blaisdell, scour time, and scour depth solutions because those NOF values are based on comparisons of scour times and depths, not scour rates. NOF values based on scour rate could have been calculated for those solution methods to allow a direct comparison, but the results can be predicted without completing the exercise. Comparison of NOF values calculated from scour times would show the scour time method to provide the best results, NOF values calculated from scour depths would show the scour depth method to perform best, and NOF values calculated from scour rates would show the linear regression method to perform best because each particular method is optimized to produce the best fit using the respective objective. Thus, comparison of NOF values is not useful for determining a preferred solution method.

The strongest argument for the use of the linear regression of scour rate data is offered in figure 3, which shows that the correlation of the scour rate (k_d) and critical shear (τ_c) parameters is significantly better for the linear regression method than for all other methods. This is consistent with broad empirical evidence that soils with high initial resistance to erosion will also exhibit slower growth of the rates of erosion as stresses increase (e.g., Briaud et al., 2001; Hanson and Simon, 2001; Wan and Fell, 2004). The high correlation of these parameters also enables effective classification of soils into erodibility categories.

Although the observed erosion rate versus applied stress curves for most of these tests were linear, about half of the tests exhibited erosion rates asymptotically approaching zero at very low stress levels (e.g., fig. 11, test 6). If the application of interest is in a stress range corresponding to the linear data, then to obtain τ_c and k_d values that best represent the linear behavior, regression analysis should be conducted using only the linear data, and the intercept of the resulting linear relation with the zero-stress axis will define the critical shear stress. This requires subjective, manual intervention to separate the linear and nonlinear sections. Exclusion of such data will always lead to an increase of τ_c and k_d. The data collected in this study were reanalyzed with manual exclusion of nonlinear data at very low stresses, but the effect on results was generally small and did not affect the conclusions of the study.

Conclusions

Methods used for analyzing data obtained from the submerged jet erosion test (JET) were examined using data obtained from a series of carefully conducted JETs on four soils compacted across a range of water contents. Nonlinear solution methods had the ability to produce good fits to data obtained from individual tests, but consistency of erodibility parameters across multiple tests was poor due to the nonlinear models apparently overfitting themselves to noise in the individual test data. Tests conducted in different ranges of applied shear stress were unable to demonstrate the "final region" erosion behavior predicted by the Wilson model. An exponential-linear erosion model was developed during the study that was similar to the initial and linear regions of the Wilson model without the final region, and this model was able to provide good fits to individual JETs but also produced inconsistent results across multiple tests.

Determining the k_d and τ_c parameters of the linear excess stress equation using a simple linear regression of average scour rate versus average applied stress offers a good combination of simplicity and consistency of results. This method provides the best correlation of k_d and τ_c, which is of significant value for ranking and classifying the erodibility of soils. When large ranges of shear stress are expected to occur in a specific application, the potential for nonlinear erosion behavior still makes it advisable to conduct JETs in the expected stress range to avoid the need to extrapolate erosion rates at untested stresses. Manual evaluation of collected data should be performed so that linear regressions exclude data points collected in low-stress regions where erosion rates may deviate from linear behavior and asymptotically approach zero.

Previous investigators have proposed various inverse power curve relations between k_d and τ_c and associated ranges of k_d and τ_c values that define descriptive erodibility categories spanning about five orders of magnitude of k_d (e.g. Hanson and Simon, 2001). Many of these studies relied on the Blaisdell solution method or other methods that tend to produce significantly different results from the linear regression method used in this study. This study covered only about three orders of magnitude of k_d, so it does not provide sufficient data to propose a new erodibility classification scheme. This would be a valuable topic for future research.

Acknowledgements

This work was funded by the Technology Development Program of the U.S. Bureau of Reclamation (USBR) Dam Safety Office. Blake Armstrong of the USBR Geotechnical Laboratory and Field Support Group provided peer review and coordinated the soil properties tests performed by outside laboratories and USBR staff. Soil erodibility tests were performed in the USBR laboratory by Kelsi Whitesell, Kent Scott, and Carolyne Bocovich.

Nomenclature

a = numerical exponent greater than zero in nonlinear excess stress equation

b_0 = erosion rate parameter of Wilson equation

b_1 = reference stress parameter of Wilson equation

c_v = turbulence coefficient of variation

e = base of natural logarithms, approximately 2.7183

K = reference erosion rate in dimensionless excess stress equation; the erosion rate when applied stress $t = 2t_c$.

k_d = detachment rate coefficient

N = number of observations in a data set

NOF = normalized objective function

p = number of parameters in a statistical model

R^2 = coefficient of determination

R^2_{adj}= adjusted coefficient of determination

SS_{res} = residual sum of squares

SS_{tot} = total sum of squares

WC_{opt} = optimum water content

x_i = observed value

X_a = mean of a set of observed values

y_i = predicted value

Greek Letters

e_r = erosion rate, volume per unit area per unit time

$?_{d,max}$ = dry unit weight of soil compacted at optimum water content

$?_d$ = dry density

t = applied shear stress

t_c = critical shear stress

References

Abdel-Rahman, N. M. (1963). The effects of flowing water on cohesive beds. PhD diss. Mitteilungen No. 56. Zurich, Switzerland: ETH Zurich.

Akinola, A. I., Wynn-Thompson, T., Olgun, C. G., Cuceoglu, F., & Mostaghimi, S. (2018). Influence of sample holding time on the fluvial erosion of remolded cohesive soils. *J. Hydraul. Eng., 144*(8), 04018049. https://doi.org/10.1061/(ASCE)HY.1943-7900.0001504

Akinola, A. I., Wynn-Thompson, T., Olgun, C. G., Mostaghimi, S., & Eick, M. J. (2019). Fluvial erosion rate of cohesive streambanks is directly related to the difference in soil and water temperatures. *J. Environ. Qual., 48*(6), 1741-1748. https://doi.org/10.2134/jeq2018.10.0385

Al-Madhhachi, A.-S. T., Hanson, G. J., Fox, G. A., Tyagi, A. K., & Bulut, R. (2013a). Deriving parameters of a fundamental detachment model for cohesive soils from flume and jet erosion tests. *Trans. ASABE, 56*(2), 489-504. https://doi.org/10.13031/2013.42669

Al-Madhhachi, A.-S. T., Hanson, G. J., Fox, G. A., Tyagi, A. K., & Bulut, R. (2013b). Measuring soil erodibility using a laboratory “mini” JET. *Trans. ASABE, 56*(3), 901-910. https://doi.org/http://dx.doi.org/10.13031/trans.56.9742

Ariathurai, R., & Arulanandan, K. (1978). Erosion rates of cohesive soils. *J. Hydraul. Div., 104*(2), 279-283. https://doi.org/10.1061/JYCEAJ.0004937

Arulanandan, K., Gillogley, E., & Tully, R. (1980). Development of a quantitative method to predict critical shear stress and rate of erosion of natural undisturbed cohesive soils. Technical Report GL-80-5. Vicksburg, MS: U.S. Army Corp of Engineers, Waterways Experiment Station.

ASTM (1995). D5852: Standard test method for erodibility determination in the field or in the laboratory by the jet index method (withdrawn 2016). West Conshohocken, PA: ASTM

ASTM. (2020). *Annual book of ASTM Standards*. West Conshohocken, PA: ASTM.

Blaisdell, F. W., Hebaus, G. G., & Anderson, C. L. (1981). Ultimate dimensions of local scour. *J. Hydraul. Div., 107*(3), 327-337. https://doi.org/10.1061/JYCEAJ.0005630

Briaud, J. L., Ting, F. C., Chen, H. C., Cao, Y., Han, S. W., & Kwak, K. W. (2001). Erosion function apparatus for scour rate predictions. *J. Geotech. Geoenviron. Eng., 127*(2), 105-113. https://doi.org/10.1061/(ASCE)1090-0241(2001)127:2(105)

Carlson E., J., & Enger. P., F. (1963). Studies of tractive forces of cohesive soils in earth canals. Report No. HYD-504. Denver, CO: U.S. Bureau of Reclamation, Hydraulic Laboratory.

Cossette, D., Mazurek, K. A., & Rennie, C. D. (2012). Critical shear stress from varied method of analysis of a submerged circular turbulent impinging jet test for determining erosion resistance of cohesive soils. *Proc. 6th Intl. Conf. on Scour and Erosion.*

Criswell, D. T., Al-Madhhachi, A. T., Fox, G. A., & Miller, R. B. (2016). Deriving erodibility parameters of a mechanistic detachment model for gravels. *Trans. ASABE, 59*(1), 145-151. https://doi.org/10.13031/trans.59.11490

Daly, E. R., Fox, G. A., Miller, R. B., & Al-Madhhachi, A.-S. T. (2013). A scour depth approach for deriving erodibility parameters from jet erosion tests. *Trans. ASABE, 56*(6), 1343-1351. https://doi.org/10.13031/trans.56.10350

Daly, E. R., Miller, R. B., & Fox, G. A. (2015). Modeling streambank erosion and failure along protected and unprotected composite streambanks. *Adv. Water Resour., 81*, 114-127. https://doi.org/10.1016/j.advwatres.2015.01.004

Daly, E. R., Fox, G. A., & Fox, A. K. (2016). Correlating site-scale erodibility parameters from jet erosion tests to soil physical properties. Trans. ASABE, 59(1):115-128. http://doi.org/10.13031/trans.59.11309

Dillaha III, T. A., & Beasley, D. B. (1983). Distributed parameter modeling of sediment movement and particle size distributions. *Trans. ASAE, 26*(6), 1766-1772. https://doi.org/10.13031/2013.33840

Dunn, I. S. (1959). Tractive resistance of cohesive channels. *J. Soil Mech. Foundations Div., 85*(3), 1-24.

Einstein, H. A., & El-Samni, E.-S. A. (1949). Hydrodynamic forces on a rough wall. *Rev. Mod. Phys., 21*(3), 520-524. https://doi.org/10.1103/RevModPhys.21.520

Elliot, W. J., Liebenow, A. M., Laflen, J. M., & Kohl, K. D. (1989). A compendium of soil erodibility data from WEPP cropland soil field erodibility experiments 1987 and 1988. NSERL Report No. 3. West Lafayette, IN: USDA-ARS National Soil Erosion Research Laboratory.

Foster, G. R., Meyer, L. D., & Onstad, C. A. (1977). An erosion equation derived from basic erosion principles. *Trans. ASAE, 20*(4), 678-682. https://doi.org/10.13031/2013.35627

Gao, X., Wang, Q., & Ma, G. (2019). Experimental investigation on the erosion threshold and rate of gravel and silty clay mixtures. *Trans. ASABE, 62*(4), 867-875. https://doi.org/10.13031/trans.13290

Grissinger, E. H. (1966). Resistance of selected clay systems to erosion by water. *Water Resour. Res., 2*(1), 131-138. https://doi.org/10.1029/WR002i001p00131

Hanson, G. J. (1989). Channel erosion study of two compacted soils. *Trans. ASAE, 32*(2), 485-490. https://doi.org/10.13031/2013.31030

Hanson, G. J. (1990). Surface erodibility of earthen channels at high stresses: Part II. Developing an *in situ* testing device. *Trans. ASAE, 33*(1), 132-137. https://doi.org/10.13031/2013.31306

Hanson, G. J. (1991). Development of a jet index to characterize erosion resistance of soils in earthen spillways. *Trans. ASAE, 34*(5), 2015-2020. https://doi.org/10.13031/2013.31831

Hanson, G. J. (1996). Investigating soil strength and stress-strain indices to characterize erodibility. *Trans. ASAE, 39*(3), 883-890. https://doi.org/10.13031/2013.27573

Hanson, G. J., & Cook, K. R. (1997). Development of excess shear stress parameters for circular jet testing. ASAE Paper No. 972227. St. Joseph, MI: ASAE.

Hanson, G. J., & Cook, K. R. (2004). Apparatus, test procedures, and analytical methods to measure soil erodibility *in situ*. *Appl. Eng. Agric., 20*(4), 455-462. https://doi.org/10.13031/2013.16492

Hanson, G. J., & Hunt, S. L. (2007). Lessons learned using laboratory JET method to measure soil erodibility of compacted soils. *Appl. Eng. Agric., 23*(3), 305-312. https://doi.org/10.13031/2013.22686

Hanson, G. J., & Simon, A. (2001). Erodibility of cohesive streambeds in the loess area of the midwestern USA. *Hydrol. Proc., 15*(1), 23-38. https://doi.org/10.1002/hyp.149

Hanson, G. J., Cook, K. R., & Simon, A. (2002). Non-vertical jet testing of cohesive streambank materials. ASAE Paper No. 022119. St. Joseph, MI: ASAE.

Hanson, G. J., Robinson, K. M., & Temple, D. M. (1990). Pressure and stress distributions due to a submerged impinging jet. *Proc. National Conf. Hydraulic Engineering* (pp. 525-530). Reston, VA: ASCE.

Kamphuis, J. W., & Hall, K. R. (1983). Cohesive material erosion by unidirectional current. *J. Hydraul. Eng., 109*(1), 49-61. https://doi.org/10.1061/(ASCE)0733-9429(1983)109:1(49)

Khanal, A., & Fox, G. A. (2020). Soil moisture impacts linear and nonlinear erodibility parameters from jet erosion tests. *Trans. ASABE, 63*(4), 1123-1131. https://doi.org/10.13031/trans.13835

Khanal, A., Fox, G. A., & Al-Madhhachi, A. T. (2016b). Variability of erodibility parameters from laboratory mini jet erosion tests. *J. Hydrol. Eng., 21*(10), 04016030. https://doi.org/10.1061/(ASCE)HE.1943-5584.0001404

Khanal, A., Klavon, K. R., Fox, G. A., & Daly, E. R. (2016a). Comparison of linear and nonlinear models for cohesive sediment detachment: Rill erosion, hole erosion test, and streambank erosion studies. *J. Hydraul. Eng., 142*(9), 04016026. https://doi.org/10.1061/(ASCE)HY.1943-7900.0001147

Lin, Q., & Wu, W. (2013). A one-dimensional model of mixed cohesive and non-cohesive sediment transport in open channels. *J. Hydraul. Res., 51*(5), 506-517. https://doi.org/10.1080/00221686.2013.812046

Luthi, M. (2011). A modified hole erosion test (HET-P) to study erosion characteristics of soil. MS thesis. Vancouver, BC, Canada: University of British Columbia.

Lyle, W. M., & Smerdon, E. T. (1965). Relation of compaction and other soil properties to erosion resistance of soils. *Trans. ASAE, 8*(3), 419-422. https://doi.org/10.13031/2013.40536

Marot, D., Regazzoni, P.-L., & Wahl, T. (2011). Energy-based method for providing soil surface erodibility rankings. *J. Geotech. Geoenviron. Eng., 137*(12), 1290-1293. https://doi.org/10.1061/(ASCE)GT.1943-5606.0000538

McNeil, J., Taylor, C., & Lick, W. (1996). Measurements of erosion of undisturbed bottom sediments with depth. *J. Hydraul. Eng., 122*(6), 316-324. https://doi.org/10.1061/(ASCE)0733-9429(1996)122:6(316)

Nguyen, V.-N., Courivaud, J.-R., Pinettes, P., Souli, H., & Fleureau, J.-M. (2017). Using an improved jet-erosion test to study the influence of soil parameters on the erosion of a silty soil. *J. Hydraul. Eng., 143*(8), 04017018. https://doi.org/10.1061/(ASCE)HY.1943-7900.0001305

Partheniades, E. (1965). Erosion and deposition of cohesive soils. *J. Hydraul. Div., 91*(1), 105-139. https://doi.org/10.1061/JYCEAJ.0001165

Partheniades, E., & Paaswell, R. E. (1968). Erosion of cohesive soil and channel stabilization. Civil Engineering Report No. 19. Buffalo, ,NY: New York State University.

Riha, J., & Jandora, J. (2015). Pressure conditions in the hole erosion test. *Canadian Geotech. J., 52*, 114-119. https://doi.org/10.1139/cgj-2013-0474

Simon, A., Thomas, R. E., & Klimetz, L. (2010). Comparison and experiences with field techniques to measure critical shear stress and erodibility of cohesive deposits. *Proc. 2nd Joint Federal Interagency Conf.* Reston, VA: USGS.

Smerdon, E. T., & Beasley, R. P. (1959). The tractive force theory applied to stability of open channels in cohesive soils. Research Bulletin 715. Columbia, MO: University of Missouri Agricultural Experiment Station.

Stein, O. R., & Nett, D. D. (1997). Impinging jet calibration of excess shear sediment detachment parameters. *Trans. ASAE, 40*(6), 1573-1580. https://doi.org/10.13031/2013.21421

Stein, O. R., Julien, P. Y., & Alonso, C. V. (1993). Mechanics of jet scour downstream of a headcut. *J. Hydraul. Res., 31*(6), 723-738. https://doi.org/10.1080/00221689309498814

Temple, D. M. (1985). Stability of grass-lined channels following mowing. *Trans. ASAE, 28*(3), 750-754. https://doi.org/10.13031/2013.32332

Van Damme, M., & Riteco, J. (2018). Comparing soil erodibility predictions against the fundamental understanding of erosion. *Proc. 3rd Intl. Conf. on Protection against Overtopping.*

Van Klaveren, R. W., & McCool, D. K. (1987). Hydraulic erosion resistance of thawing soil. ASAE Paper No. 87-2602. St. Joseph, MI: ASAE.

Wahl, T. L., Regazzini, P.-L., & Erdogan, Z. (2008). Determining erosion indices of cohesive soils with the hole erosion test and jet erosion test. Dam Safety Technology Development Report DSO-08-05. Denver, CO: U.S. Bureau of Reclamation.

Walder, J. S. (2016). Dimensionless erosion laws for cohesive sediment. *J. Hydraul. Eng., 142*(2), 04015047. https://doi.org/10.1061/(ASCE)HY.1943-7900.0001068

Wan, C. F., & Fell, R. (2004). Investigation of rate of erosion of soils in embankment dams. *J. Geotech. Geoenviron. Eng., 130*(4), 373-380. https://doi.org/10.1061/(ASCE)1090-0241(2004)130:4(373)

Wilson, B. N. (1993a). Development of a fundamentally based detachment model. *Trans. ASAE, 36*(4), 1105-1114. https://doi.org/10.13031/2013.28441

Wilson, B. N. (1993b). Evaluation of a fundamentally based detachment model. *Trans. ASAE, 36*(4), 1115-1122. https://doi.org/10.13031/2013.28442

Abdel-Rahman, N. M. (1963). The effects of flowing water on cohesive beds. PhD diss. Mitteilungen No. 56. ETH Zurich.

Akinola, A. I., Wynn-Thompson, T., Olgun, C. G., Cuceoglu, F., & Mostaghimi, S. (2018). Influence of sample holding time on the fluvial erosion of remolded cohesive soils. *J. Hydraul. Eng., 144*(8), 04018049. doi:https://doi.org/10.1061/(ASCE)HY.1943-7900.0001504

Akinola, A. I., Wynn-Thompson, T., Olgun, C. G., Mostaghimi, S., & Eick, M. J. (2019). Fluvial erosion rate of cohesive streambanks is directly related to the difference in soil and water temperatures. *JEQ, 48*(6), 1741-1748. doi:https://doi.org/10.2134/jeq2018.10.0385

Al-Madhhachi, A.-S. T., Hanson, G. J., Fox, G. A., Tyagi, A. K., & Bulut, R. (2013a). Deriving parameters of a fundamental detachment model for cohesive soils from flume and jet erosion tests.

Trans. ASABE, 56(2), 489-504. doi:https://doi.org/10.13031/2013.42669

Al-Madhhachi, A.-S. T., Hanson, G. J., Fox, G. A., Tyagi, A. K., & Bulut, R. (2013b). Measuring soil erodibility using a laboratory "mini" JET. *Trans. ASABE, 56*(3), 901-910. doi:https://doi.org/http://dx.doi.org/10.13031/trans.56.9742

Ariathurai, R., & Arulanandan, K. (1978). Erosion rates of cohesive soils. *J. Hydraul. Div., 104*(2), 279-283. doi:https://doi.org/10.1061/JYCEAJ.0004937

Arulanandan, K., Gillogley, E., & Tully, R. (1980). Development of a quantitative method to predict critical shear stress and rate of erosion of natural undisturbed cohesive soils. USACE, Waterways Experiment Station Technical Report, GL-80-5. Vicksburg, MS.

ASTM. (2020). *Annual book of ASTM Standards, Section 4: Construction* (Vol. 04.08). Philadelphia, PA: ASTM.

Blaisdell, F. W., Hebaus, G. G., & Anderson, C. L. (1981). Ultimate dimensions of local scour. *J. Hydraul. Div., 107*(3), 327-337. doi:https://doi.org/10.1061/JYCEAJ.0005630

Briaud, J. L., Ting, F. C., Chen, H. C., Cao, Y., Han, S. W., & Kwak, K. W. (2001). Erosion function apparatus for scour rate predictions. *J. Geotech. Geoenviron. Eng., 127*(2), 105-113. doi:https://doi.org/10.1061/(ASCE)1090-0241(2001)127:2(105)

Carlson E., J., & Enger. P., F. (1963). Studies of tractive forces of cohesive soils in earth canals. Hydraulic Laboratory Report No. HYD-504. Denver, CO: Bureau of Reclamation.

Cossette, D., Mazurek, K. A., & Rennie, C. D. (2012). Critical shear stress from varied method of analysis of a submerged circular turbulent impinging jet test for determining erosion resistance of cohesive soils. *Proc. 6th Int. Conf. on Scour and Erosion.*

Criswell, D. T., Al-Madhhachi, A. T., Fox, G. A., & Miller, R. B. (2016). Deriving erodibility parameters of a mechanistic detachment model for gravels. *Trans. ASABE, 59*(1), 145-151. doi:https://doi.org/10.13031/trans.59.11490

Daly, E. R., Fox, G. A., & Fox, A. K. (2016). Correlating site-scale erodibility parameters from jet erosion tests to soil physical properties. *Trans. ASABE, 59*(1), 115-125. doi:http://doi.org/10.13031/trans.59.11309

Daly, E. R., Fox, G. A., Miller, R. B., & Al-Madhhachi, A.-S. T. (2013). A scour depth approach for deriving erodibility parameters from jet erosion tests. *Trans. ASABE, 56*(6), 1343-1351. doi:https://doi.org/10.13031/trans.56.10350

Daly, E. R., Miller, R. B., & Fox, G. A. (2015). Modeling streambank erosion and failure along protected and unprotected composite streambanks. *Adv. Water Resour., 81*, 114-127. doi:https://doi.org/10.1016/j.advwatres.2015.01.004

Dillaha III, T. A., & Beasley, D. B. (1983). Distributed parameter modeling of sediment movement and particle size distributions. *Trans. ASAE, 26*(6), 1766-1772. doi:https://doi.org/10.13031/2013.33840

Dunn, I. S. (1959). Tractive resistance of cohesive channels. *J. Soil Mech. Foundations Div., 85*(3), 1-24.

Einstein, H. A., & El-Samni, E.-S. A. (1949). Hydrodynamic forces on a rough wall. *Rev. Mod. Phys., 21*(3), 520-524. doi:https://doi.org/10.1103/RevModPhys.21.520

Elliot, W. J., Liebenow, A. M., Laflen, J. M., & Kohl, K. D. (1989). A compendium of soil erodibility data from WEPP cropland soil field erodibility experiments 1987 and 1988. NSERL Report No. 3. Columbus: Ohio State University and USDA Agricultural Research Service.

Foster, G. R., Meyer, L. D., & Onstad, C. A. (1977). An erosion equation derived from basic erosion principles. *Trans. ASAE, 20*(4), 678-682. doi:https://doi.org/10.13031/2013.35627

Gao, X., Wang, Q., & Ma, G. (2019). Experimental investigation on the erosion threshold and rate of gravel and silty clay mixtures. *Trans. ASABE, 62*(4), 867-875. doi:https://doi.org/10.13031/trans.13290

Grissinger, E. H. (1966). Resistance of selected clay systems to erosion by water. *Water Resour. Res., 2*(1), 131-138. doi:https://doi.org/10.1029/WR002i001p00131

Hanson, G. J. (1989). Channel erosion study of two compacted soils. *Trans. ASAE, 32*(2), 485-490. doi:https://doi.org/10.13031/2013.31030

Hanson, G. J. (1990). Surface erodibility of earthen channels at high stresses part II - developing an in situ testing device. *Trans. ASAE, 33*(1), 132-137. doi:https://doi.org/10.13031/2013.31306

Hanson, G. J. (1996). Investigating soil strength and stress-strain indices to characterize erodibility. *Trans. ASAE, 39*(3), 883-890. doi:https://doi.org/10.13031/2013.27573

Hanson, G. J., & Cook, K. R. (1997). Development of excess shear stress parameters for circular jet testing. ASAE Paper No. 972227. St. Joseph, MI: ASAE.

Hanson, G. J., & Cook, K. R. (2004). Apparatus, test procedures, and analytical methods to measure soil erodibility in situ. *Appl. Eng. Agric., 20*(4), 455-462. doi:https://doi.org/10.13031/2013.16492

Hanson, G. J., & Hunt, S. L. (2007). Lessons learned using laboratory JET method to measure soil erodibility of compacted soils. *Appl. Eng. Agric., 23*(3), 305-312. doi:https://doi.org/10.13031/2013.22686

Hanson, G. J., & Simon, A. (2001). Erodibility of cohesive streambeds in the loess area of the midwestern USA. *Hydrol. Process., 15*(1), 23-38. doi:https://doi.org/10.1002/hyp.149

Hanson, G. J., Cook, K. R., & Simon, A. (2002). Non-vertical jet testing of cohesive streambank materials. ASAE Paper No. 022119. St. Joseph, MI: ASAE.

Hanson, G. J., Robinson, K. M., & Temple, D. M. (1990). Pressure and stress distributions due to a submerged impinging jet. *Proc. National Conf. Hydraulic Engineering* (pp. 525-530). ASCE.

Hanson, G. J., Temple, D. M., Hunt, S. L., & Tejral, R. (2011). Development and characterization of soil material parameters for embankment breach. *Appl. Eng. Agric., 27*(4), 587-595. doi:https://doi.org/10.13031/2013.38205

Kamphuis, J. W., & Hall, K. R. (1983). Cohesive material erosion by unidirectional current. *J. Hydraul. Eng., 109*(1), 49-61. doi:https://doi.org/10.1061/(ASCE)0733-9429(1983)109:1(49)

Khanal, A., & Fox, G. A. (2020). Soil moisture impacts linear and nonlinear erodibility parameters from jet erosion tests. *Trans. ASABE, 63*(4), 1123-1131. doi:https://doi.org/10.13031/trans.13835

Khanal, A., Fox, G. A., & Al-Madhhachi, A. T. (2016b). Variability of erodibility parameters from laboratory mini jet erosion tests. *J. Hydrol. Eng., 21*(10), 04016030. doi:https://doi.org/10.1061/(ASCE)HE.1943-5584.0001404

Khanal, A., Klavon, K. R., Fox, G. A., & Daly, E. R. (2016a). Comparison of linear and nonlinear models for cohesive sediment detachment: Rill erosion, hole erosion test, and streambank erosion studies. *J. Hydraul. Eng., 142*(9), 04016026. doi:https://doi.org/10.1061/(ASCE)HY.1943-7900.0001147

Lin, Q., & Wu, W. (2013). A one-dimensional model of mixed cohesive and non-cohesive sediment transport in open channels. *J. Hydraul. Res., 51*(5), 506-517. doi:https://doi.org/10.1080/00221686.2013.812046

Luthi, M. (2011). A modified hole erosion test (HET-P) to study erosion characteristics of soil. MS thesis. Vancouver: Univ. of British Columbia.

Lyle, W. M., & Smerdon, E. T. (1965). Relation of compaction and other soil properties to erosion resistance of soils. *Trans. ASAE, 8*(3), 419-422. doi:https://doi.org/10.13031/2013.40536

Marot, D., Regazzoni, P.-L., & Wahl, T. (2011). Energy-based method for providing soil surface erodibility rankings. *J. Geotech. Geoenviron. Eng., 137*(12), 1290-1293. doi:https://doi.org/10.1061/(ASCE)GT.1943-5606.0000538

McNeil, J., Taylor, C., & Lick, W. (1996). Measurements of erosion of undisturbed bottom sediments withâ€‰depth. *J. Hydraul. Eng., 122*(6), 316-324. doi:https://doi.org/10.1061/(ASCE)0733-9429(1996)122:6(316)

Nguyen, V.-N., Courivaud, J.-R., Pinettes, P., Souli, H., & Fleureau, J.-M. (2017). Using an improved jet-erosion test to study the influence of soil parameters on the erosion of a silty soil. *J. Hydraul. Eng., 143*(8), 04017018. doi:https://doi.org/10.1061/(ASCE)HY.1943-7900.0001305

Partheniades, E. (1965). Erosion and deposition of cohesive soils. *J. Hydraul. Div., 91*(1), 105-139. doi:https://doi.org/10.1061/JYCEAJ.0001165

Partheniades, E., & Paaswell, R. E. (1968). Erosion of cohesive soil and channel stabilization. Civil Eng. Report No. 19. Buffalo: New York State University.

Simon, A., Thomas, R. E., & Klimetz, L. (2010). Comparison and experiences with field techniques to measure critical shear stress and erodibility of cohesive deposits. *Proc. 2nd Joint Federal Interagency Conf.* USGS.

Smerdon, E. T., & Beasley, R. P. (1959). The tractive force theory applied to stability of open channels in cohesive soils. Research Bulletin 715. Univ. Missouri Ag. Exp. Station.

Smith, J., Perkey, D., & Priestas, A. (2015). Erosion thresholds and rates for sand-mud mixtures. *Proc. 13th Int. Conf. on Cohesive Sediment Transport Process.*

Stein, O. R., & Nett, D. D. (1997). Impinging jet calibration of excess shear sediment detachment parameters. *Trans. ASAE, 40*(6), 1573-1580. doi:https://doi.org/10.13031/2013.21421

Stein, O. R., Julien, P. Y., & Alonso, C. V. (1993). Mechanics of jet scour downstream of a headcut. *J. Hydraul. Res., 31*(6), 723-738. doi:https://doi.org/10.1080/00221689309498814

Temple, D. M. (1985). Stability of grass lined channels following mowing. *Trans. ASAE, 28*(3), 750-754. doi:https://doi.org/10.13031/2013.32332

Van Damme, M., & Riteco, J. (2018). Comparing soil erodibility predictions against the fundamental understanding of erosion. *Proc. 3rd Int. Conf. on Protection Against Overtopping.*

Van Klaveren, R. W., & McCool, D. K. (1987). Hydraulic erosion resistance of thawing soil. ASAE Paper No. 87-2602. St. Joseph, MI: ASAE.

Wahl, T. L., Regazzoni, P.-L., & Erdogan, Z. (2008). Determining erosion indices of cohesive soils with the hole erosion test and jet erosion test. Dam Safety Technology Development Report DSO-08-05. Denver, CO: U.S. Dept. of the Interior, Bureau of Reclamation.

Walder, J. S. (2016). Dimensionless erosion laws for cohesive sediment. *J. Hydraul. Eng., 142*(2), 04015047. doi:https://doi.org/10.1061/(ASCE)HY.1943-7900.0001068

Wan, C. F., & Fell, R. (2004). Investigation of rate of erosion of soils in embankment dams. *J. Geotech. Geoenviron. Eng., 130*(4), 373-380. doi:https://doi.org/10.1061/(ASCE)1090-0241(2004)130:4(373)

Wilson, B. N. (1993a). Development of a fundamentally based detachment model. *Trans. ASAE, 36*(4), 1105-1114. doi:https://doi.org/10.13031/2013.28441

Wilson, B. N. (1993b). Evaluation of a fundamentally based detachment model. *Trans. ASAE, 36*(4), 1115-1122. doi:https://doi.org/10.13031/2013.28442

American Society of Agricultural and Biological Engineers

2950 Niles Road, St. Joseph, MI 49085
Phone: +12694290300 Fax: +12694293852